Doctoral Dissertation

Mechanism of Liquid-Liquid Phase Separation of Temperature response Polyampholyte and Its Applications

Tomoka HIROSE

Supervisor: Kazuaki MATSUMURA

Graduate School of Advanced Science and Technology

Japan Advanced Institute of Science and Technology

Materials Science

June 2024

Abstract

Tomoka Hirose

Polyampholytes, a class of polyelectrolytes characterized by the presence of both anionic and cationic groups, demonstrate unique pH and temperature responsiveness through interactions the polymers and their surrounding solutions or among the polymers' own functional groups. Such responsiveness enables polyampholytes to undergo phase transitions, making them invaluable in diverse applications ranging from smart materials to biomedical engineering. Due to its high biocompatibility, it is being actively researched as an intelligent material suitable for biomaterials such as drug delivery systems (DDS). Understanding the mechanisms driving these stimulus-responsive phase transitions is crucial for the optimization of polyampholyte-based materials, as it informs the design and functionalization strategies that tailor their properties to specific applications. Furthermore, in recent years, attention has been focused on the behavior of liquid-liquid phase separation (LLPS) in living organisms such as organelles without membranes. This interest is driven by the role of LLPS in critical life processes, including metabolism, where it facilitates the compartmentalization of biochemical reactions without the need for physical barriers. Polyampholytes are also being studied as model compounds for proteins, offering insights into the molecular dynamics underlying phase separation biology.

In this study, I explore the synthesis and evaluation of ampholyte polymers that exhibit both liquid-liquid phase separation (LLPS) behavior and temperature responsiveness. We confirmed that by introducing a benzene ring into an ampholyte polymer that causes phase separation behavior due to electrostatic interactions, stable phase separation behavior can be induced even in salt solvents. Multi-scale measurements revealed that the benzene rings play a crucial role during droplet formation and growth stages likely due to the π-π interaction, thereby stabilizing LLPS behavior. Leveraging the temperature responsiveness of these polymers, we designed a novel DDS carrier using a composite material with photothermal properties derived from liquid metal. This approach aimed to ensure a stable, self-sufficient supply of trigger stimuli, addressing a significant limitation of current DDS technologies. Cell-based experiments demonstrated the carrier's ability to concentrate drugs effectively, suggesting its potential to minimize side effects associated with drug delivery. These findings not only contribute to our understanding of the fundamental principles governing LLPS in ampholyte polymers but also open new avenues for the development of safer, more efficient drug delivery technologies. Future research will focus on further characterizing the interaction mechanisms at play and exploring the clinical applicability of our novel DDS carrier.

Keywords: Polyampholytes, Liquid-Liquid phase separation, Drug delivery system, Temperature response polymers, Liquid metals, Biomaterials

Acknowledgment

In conducting this research, I would like to thank my supervisor, Prof. Dr. Kazuaki Matsumura, for his careful guidance and advice on everything from research preparation to writing and presentation of the paper. Also, if I had any questions, I could always go to him for advice, and he was always available to help me even though he was very busy. It is thanks to Prof. Matsumura guidance that I was able to carry out and complete my research. I would like to express my deepest gratitude and appreciation.

I would like to express my sincere gratitude to Prof. Dr. Masayuki Yamaguchi (JAIST), Assoc. Prof. Dr. Miyako Eijiro (JAIST), Prof. Dr. Motoichi Kurisawa (JAIST), and Assoc. Prof. Dr. Shinichi Yusa (University of Hyogo) for reviewing my thesis and providing useful advice.

In Chapter 2, I would like to express my gratitude to Dr. Masaru Nakada (Toray Research Center, Inc.), Mr. Hironobu Uchiyama (Toray Research Center, Inc.), and Mr. Shinya Seki(Toray Research Center, Inc.) for their great cooperation in measurements and analysis during the joint research.

In Chapter 3, I received careful and appropriate guidance from my co-researcher, Assoc. Prof. Dr. Miyako Eijiro (JAIST). I would also like to thank the members of the Miyako Laboratory for kindly lending me experimental equipment and providing guidance on how to use it.

Asst. Prof. Dr. Rajan Robin and Ms. Keiko Kawamoto of the Matsumura Laboratory taught me a lot and enabled me to carry out my research. Also, everyone in the laboratory helped me in various situations. I would like to express my deepest gratitude.

This work was supported by JST SPRING, Grant Number JPMJSP2102.

Tomoka Hirose

Table of Contents

Chapter 1
General introduction

1-1 Polyelectrolytes

Polyelectrolytes can be broadly classified into three categories[1–3]: polymers with either anions or cations, zwitterionic polymers, and amphoteric polyelectrolytes (Figure 1).

Polyelectrolytes have both polymer and electrolyte properties, and since they have dissociative groups in their repeating units, they exhibit various properties in solution due to electrostatic interactions between low molecular weight ions in solution and charged groups in the polymer chain[4,5].

When the degree of dissociation changes due to electrostatic interactions, the effective size of the chains also changes, leading to significant changes in the conformation of macromolecules such as coil-globule transitions[6]. This also significantly changes the physicochemical properties of the solution, such as its viscosity. It is possible to cause changes in physical properties by changing external conditions such as pH, temperature, and the addition of salt. Taking advantage of these properties, it can be used as a thickener[7] or dispersant[5] in industrial applications, or as a biological material. Research is being carried out on biosensors[8,9] and drug delivery systems (DDS)[10]. Materials with similar properties are often found in biomolecules, such as polyamino acids, DNA, and cell membranes[11]. In recent years, they have been studied as model compounds for proteins because they have similar properties[12].

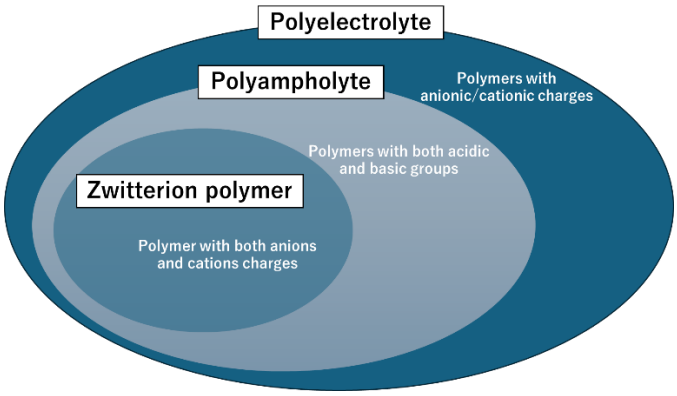

Figure.1 Polyelectrolytes and their classification

1-1-1 Zwitterionic Polymers

Among polymer electrolytes, those containing both anions and cations are called zwitterionic polymers. (Figure 2) Typical zwitterionic polymers include sulfobetaine and carboxybetaine in general, betaine-based zwitterionic polymers are often named after the anion moiety[13]. In this paper, I define zwitterionic polymers as having anionic and cationic charges in the same monomer unit to distinguish them from ampholyte polymers described later. The solution behavior of zwitterionic polymers is often opposite to that of polyelectrolytes, which is called the antipolyelectrolyte effect. Chain extension is highly dependent on the addition of low molecular weight electrolytes, chemical structure, and composition[14]. Research is being conducted into disinfectants, emulsifiers[15], and cryoprotectants[16,17].

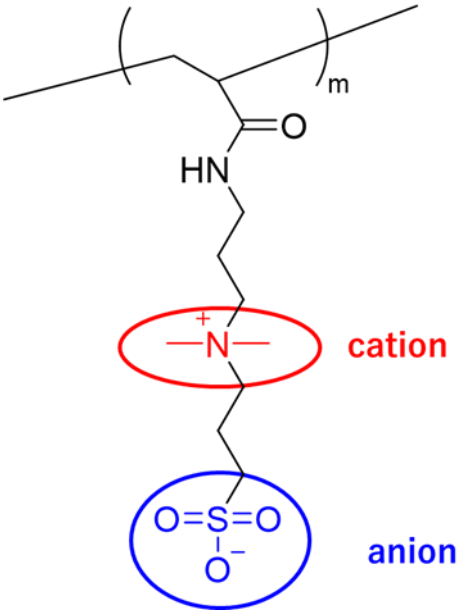

Figure 2 Sulfobetaine polymer structure

1-1-2 Polyampholytes

Ampholyte polymer is a type of polyelectrolytes, and its original definition refers to a polymer that has both acidic and basic groups[18]. For the sake of clarity in this paper, zwitterionic polymers in which different repeating units have opposite charges are referred to as ampholyte polymers. (Figure 3) Among electrolyte polymers, they have many similarities with biomolecules such as proteins, and are expected to be applied to biomaterials[12,19]. The structure and properties of ampholyte polymers are influenced by the Coulombic attraction between anionic and cationic species on different monomer units, and the response in solution is highly dependent on the chemical structure and composition of the polymer[20,21]. It has amphoteric properties, accepting protons under acidic conditions and releasing protons under basic conditions, meaning that its charge fluctuates with changes in pH[22,23]. Because it has temperature and pH responsiveness[24,25], it is being researched to be applied to biomaterials such as drug delivery systems[26,27]. Our laboratory has already reported on ampholyte polymers as cryoprotectants[16,28].

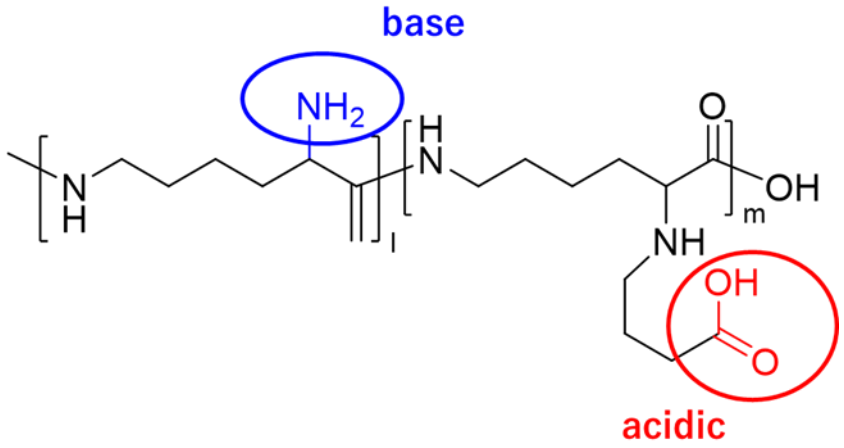

Figure 3 Structure diagram of ampholyte polymer (PLL-SA) with cryoprotective effect

1-2 Liquid-liquid phase separation

Liquid-liquid phase separation behavior (LLPS) refers to the physical phenomenon in which a solution does not mix homogeneously and separates into two phases due to changes in intermolecular interactions[29]. (Figure 4) Generally, during phase separation, a dilute phase and a concentrated phase are separated, and the concentrated phase formed at this time is called a droplet, a concentrate, a coacervate, etc[30–32]. depending on the size. This phenomenon is often observed in the natural world and has recently attracted attention as a behavior in which various intracellular metabolisms are carried out by proteins and RNA in living organisms[33–38].

Regions in cells that have no membranes but are enriched with proteins and RNA are called membraneless organelles, and they vary in size from large ones such as nucleoli and stress granules to small and temporary ones[39,40]. A state of liquid-liquid phase separation exists within cells. Those with particularly low fluidity are called gels, and those with larger sizes are sometimes called protein tertiary structures or aggregated granules[38,41,42]. This liquid-liquid phase separation in living organisms is called biological phase separation, and it has become clear that it plays an important role in biological phenomena[43–45].

During metabolism, droplets formed by LLPS contribute to the concentration and elimination of molecules depending on their affinity, which leads to the promotion and inhibition of biochemical reactions during metabolism. Furthermore, understanding LLPS is important for treatment of diseases. Aggregation of specific proteins is one of the causes of neurodegenerative diseases such as Alzheimer's disease, Parkinson's disease, and amyotrophic cord sclerosis (ALS)[46–49]. It has been revealed that such protein condensation tends to occur in the concentrated phase of liquid-liquid phase separation, and elucidation of the mechanism of liquid-liquid phase separation behavior may lead to precise control of protein aggregation inhibition or promotion.

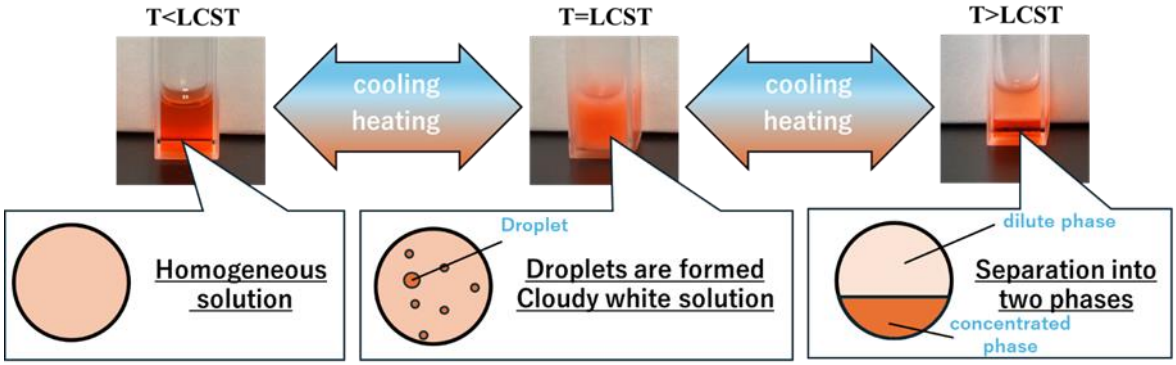

Figure 4 Liquid-liquid phase separation behavior

1-3 Temperature responsive polymer

A temperature-responsive polymer is a type of external stimulus-responsive polymer and is a polymer that changes its properties and form in response to temperature changes[50–52]. It can be divided into two types: upper critical solution temperature (UCST) type and lower critical solution temperature (LCST) type. As solubility changes with temperature changes, UCST type polymers become soluble at a certain temperature, and LCST type polymers become insolubilized at a certain temperature[53,54]. These reactions are largely caused by the affinity between the polymers and the solvent; when the interactions between polymers become dominant, they become insolubilized, and when they become recessive, they become soluble. (Figure 5) The temperature at this point is called the phase transition temperature (Tc). Examples of interactions include hydrophilic-hydrophobic interactions and electrostatic interactions. There are also various forms of change, and there are polymers that exhibit solid-liquid phase separation and polymers that exhibit liquid-liquid phase separation behavior. Taking advantage of its properties, it is a material that is being studied as a reactive material and biomaterial. Because UCST type polymers are difficult to reproduce under physiological conditions due to their characteristics, LCST type polymers are commonly studied as biomaterials.

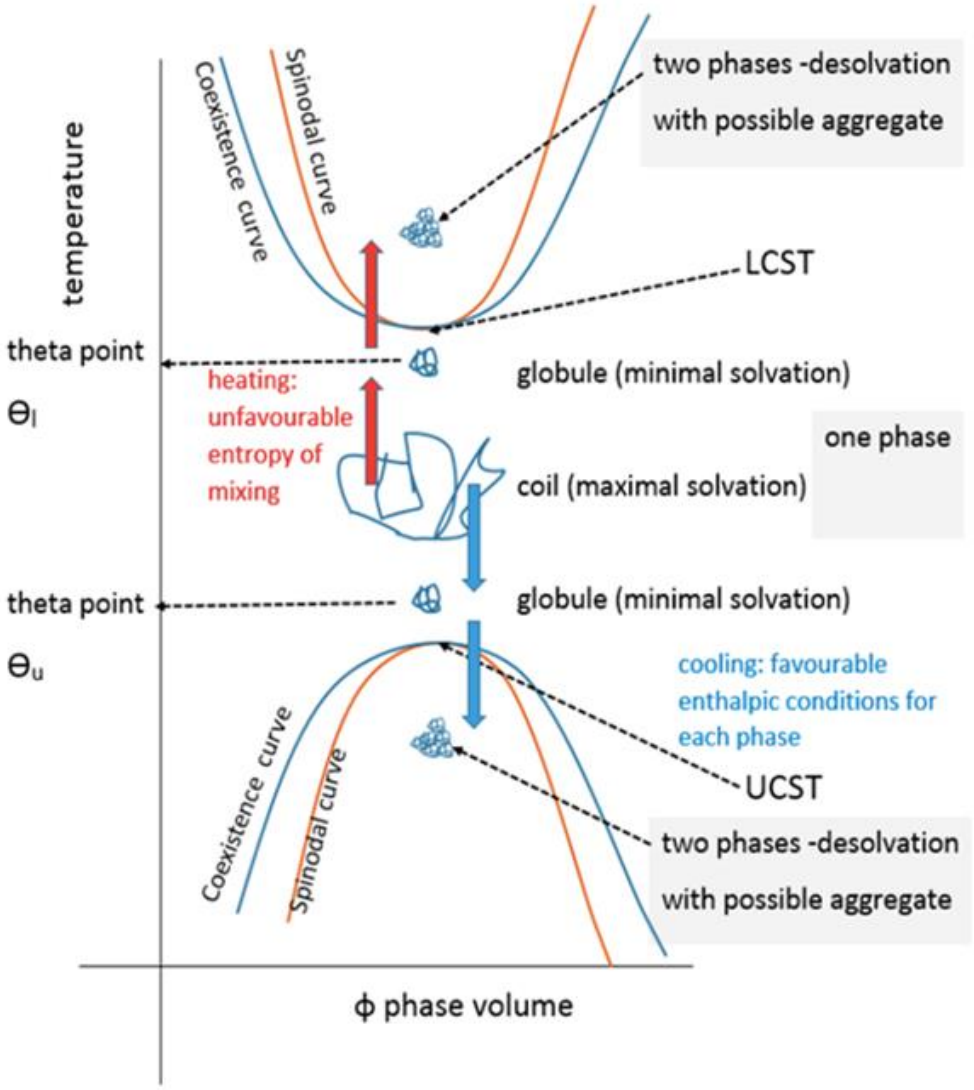

Figure 5 Illustration of phase separation behavior[54]

1-3-1 Upper Critical Solution Temperature (UCST) Polymer

Poly(allylamine-co-allylurea) (PAU) is a typical UCST type polymer. (Figure 6) PAU is a type of ureido polymer that is often used as a UCST type polymer, and is synthesized by adding potassium cyanate, a ureidation reagent, to polyallylamine[55]. In general, UCST-type phase separation behavior is often caused by hydrogen bonds, so many have a high Tc[56]. However, PAU has a wide range of Tc from 5 to 65℃ by controlling the ureidation rate and molecular weight. The phase separation behavior is due to the strong hydrogen bonding of the ureido groups, and as mentioned above, LCST-type polymers are mainly studied as biomaterials, and there are only reports that focus on UCST-type polymers[53,56]. The current situation is that the number of molecules is small. However, in recent years, research has been conducted on the application of PAU to carriers such as protein capture, temperature sensing in combination with fluorescent probes, actuators, etc[55,57].

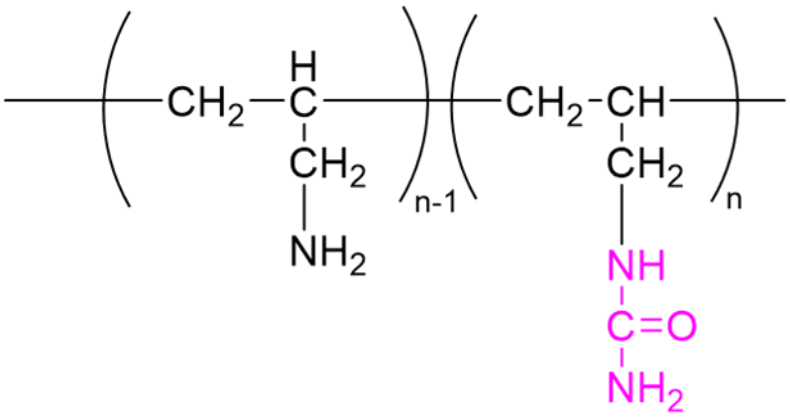

Figure 6 Structural diagram of poly (allylamine-co -allylurea) (PAU)

1-3-2 Lower Critical Solution Temperature (LCST) Polymer

Poly(N-isopropylacrylamide) (PNIPAM) is the most common LCST type polymer[58–61]. (Figure 7a) Tc of PNIPAM exhibits liquid-liquid phase separation behavior at 31-33°C due to interaction between hydrophilic and hydrophobic groups. The PNIPAM chain, which is normally in a coiled state in solution, changes its shape into a sphere as the hydrophobic interaction between the hydrophobic skeleton and the isopropyl group becomes dominant when the temperature exceeds the LCST[62]. It is a polymer that has been widely studied as a biomaterial because it has a Tc close to body temperature and has a relatively simple structure[63,64]. However, since Tc does not depend on the polymer concentration, when considering applications with different Tc, it is necessary to incorporate structural factors into the polymer structure that strengthen the interaction between the polymer and water. When applied as a carrier for biomaterials, especially DDS, it is generally used in the form of a gel [65].

Our laboratory has reported an ampholyte polymer that exhibits new LCST properties by modifying the free amino groups of ε-poly-L-lysine (PLL) with succinic anhydride (SA) (PLL-SA)[66,67] (Figure 7b). The phase separation behavior is due to electrostatic interactions and exhibits LLPS. It has been found that Tc is highly dependent on the degree of substitution of SA in the polymer and on the concentration of the polymer solution. Compared to PNIPAM, it is easier to adjust Tc, and it can be applied over a wide temperature range, including body temperature, by simply adjusting the concentration of the polymer. Furthermore, one of the raw materials, polylysine, is a material that is also used as a food additive, and its low biotoxicity is an advantage when considering it as a biomaterial[68]. However, there is a problem in that phase separation behavior is suppressed in solvents containing salts such as body fluids because electrostatic interactions are inhibited[66].

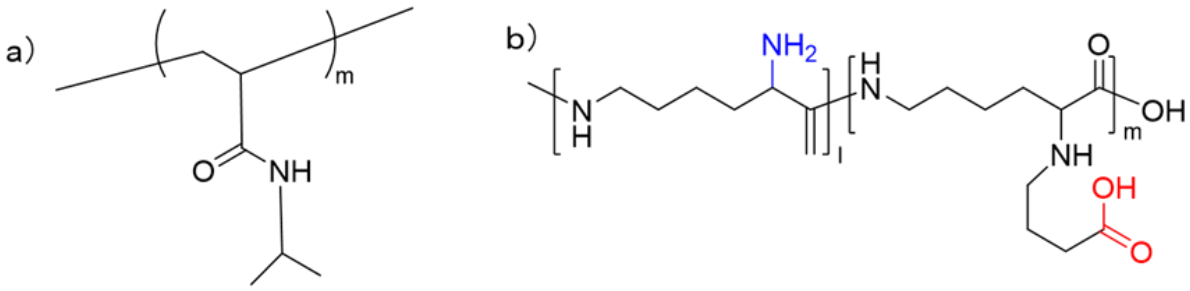

Figure 7 LCST type polymer structure (a: PNIPAM/ b: PLL-SA)

1-4 Drug Delivery System (DDS)

Drug delivery system (DDS) is a general term for technology that delivers the necessary drug to the appropriate site at the required time and is considered important in the drug discovery field from the perspective of reducing side effects and improving drug efficacy[69,70]. Generally, drugs themselves do not have site-selectivity, so in order to produce a pharmacological effect at the site of action, it is necessary to administer a large amount with consideration to absorption outside the site of action. Although large doses of drugs are the main cause of side effects, it is difficult to obtain pharmacological effects at doses below the prescribed values. DDS, which is one of the methods to solve this problem, can be classified by purpose and can be broadly divided into three categories[71]: release inhibition, absorption improvement, and target targeting. Regarding release suppression, by designing for sustained release, the drug concentration in the blood is stabilized and fluctuations are suppressed, which leads to stabilization of pharmacological effects and stabilization of side effects.

To improve absorption, the effective drug itself is modified to suit the environment at the site of action[71]. This suppresses absorption in areas other than the target site and is expected to reduce side effects[72]. Finally, regarding target orientation, the purpose of this is to design a drug to be delivered only to the target and is an important perspective for drugs that have particularly strong side effects, such as anticancer drugs[73,74]. A typical example of target-directed DDS in anticancer

drugs is the so-called Enhanced Permeability and Retention (EPR) effect. This is because the holes in the blood vessel walls surrounding cancer cells are larger than in normal cells, so it was hoped that by enlarging the size of the particles by modifying them with polymers, they would accumulate only in cancer cells[75]. DDS is being applied and researched in a wide variety of ways for each of these purposes. The most classic and familiar application of DDS is sugar-coated tablets.

In recent years, a technology called smart DDS, which has stimulus responsiveness and can improve the effectiveness of drug targeting and reduce side effects, has been actively researched[74,76–78]. Examples of smart DDS materials include liposomes, metals/metal oxides[79–81], and external stimuli-responsive polymers[74]. External stimuli-responsive polymers are a general term for polymers that change their physical properties and structure in response to the aforementioned external stimuli such as temperature, magnetism, and pH[82] (Figure 8). Many responsive polymers are being investigated as DDS carriers, depending on the treatment method, purpose, and environment of the target site. LCST type polymers are commonly used as temperature-responsive polymers[83]. While thermal stimulation is easy to supply, it is also a stimulus that is difficult to supply stably over a long period of time due to the homeostatic function of the living body. For this reason, conventional research into DDS carriers using temperature-responsive polymers has focused on how quickly and sensitively they can react[84].

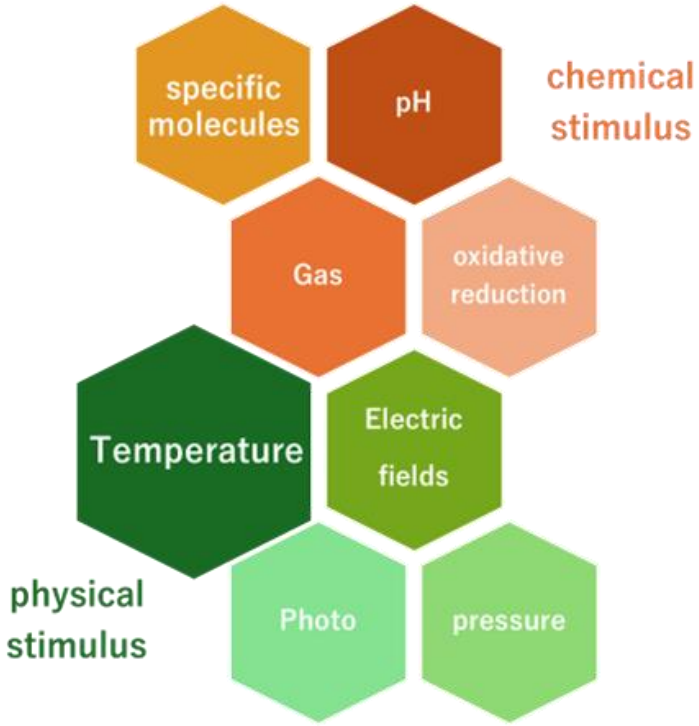

Figure 8 Typical external stimuli

1-5 Metal nanoparticles

Metal nanoparticles are materials that are being applied and researched in industrial and biological materials due to their characteristics such as localized surface plasmon resonance and catalytic properties depending on the particle size. By definition metal particles of 100 nm or less are called metal nanoparticles. There are various methods for controlling size and shape, and they are used depending on the purpose. Typical metal nanoparticles include gold and silver. Applications in many fields, including sensing and optical devices that utilize optical properties that absorb and scatter light at specific wavelengths, magnetic materials and devices that utilize magnetic properties, nanoscale materials that utilize mechanical properties, and catalysts[85]. Phototherapy in cancer treatment uses surface plasmon resonance to absorb light and generate heat, making use of its photothermal properties[86], which have been widely applied in the medical field, such as in destroying cancerous tissue. In the field of DDS, drug targeting and efficient delivery is possible by combining drugs with nanoparticles and accumulating them in tumor tissue using the EPR effect[79,86].

1-5-1 Liquid metals

It is a general term for metals that are in a liquid state at room temperature, with mercury being a typical example. It is a well-known fact that mercury has excellent physical and chemical properties, but it is also widely known that mercury is highly toxic. However, in recent years, liquid metals based on gallium have been attracting attention. In addition to the excellent properties of liquid metals, gallium-based liquid metals have low cytotoxicity, and are therefore being actively researched in the field of nanomedicine[39,87]. Since it can be made into particles by a simple method such as ultrasonication, it can also be applied as metal nanoparticles[88].

1-6 Research purpose

In this study, I synthesized a temperature-responsive ampholyte polymer that exhibits liquid-liquid phase separation behavior, incorporating hydrophobic groups to enable stable phase separation behavior even in biological environments, and explored the mechanism of its phase separation behavior. and its application to DDS. In Chapter 2, I focus on the phase separation behavior of the synthesized temperature-responsive ampholyte polymers and evaluate the characteristics of the synthesized polymers and measure the liquid-liquid phase separation behavior on various scales to determine the presence or absence of hydrophobic groups. In Chapter 3, I focused on temperature responsiveness, created a composite with liquid metal as a conventional next-generation temperature-responsive carrier, and evaluated its characteristics as a DDS carrier with two-stage responsiveness. Chapter 4 provides an overview of this research and future prospects. Chapter 4 provides an overview of this research and future prospects.

1-7 References

1. Blackman, L. D., Gunatillake, P. A., Cass, P. & Locock, K. E. S. An introduction to zwitterionic polymer behavior and applications in solution and at surfaces. *Chemical Society Reviews* vol. 48 757–770 Preprint at https://doi.org/10.1039/c8cs00508g (2019).
2. Di Noto, V., Lavina, S., Giffin, G. A., Negro, E. & Scrosati, B. Polymer electrolytes: Present, past and future. in *Electrochimica Acta* vol. 57 4–13 (Elsevier Ltd, 2011).
3. Lowe, A. B. & McCormick, C. L. Synthesis and solution properties of zwitterionic polymers. *Chem Rev* **102**, 4177–4189 (2002).
4. Fevola, M. J., Bridges, J. K., Kellum, M. G., Hester, R. D. & McCormick, C. L. pH-responsive polyzwitterions: A comparative study of acrylamide-based polyampholyte terpolymers and polybetaine copolymers. *J Appl Polym Sci* **94**, 24–39 (2004).
5. North, S. M. & Armes, S. P. Aqueous one-pot synthesis of well-defined zwitterionic diblock copolymers by RAFT polymerization: an efficient and environmentally-friendly route to a useful dispersant for aqueous pigments. *Green Chemistry* **23**, 1248–1258 (2021).
6. Wang, J. & Hui, N. Zwitterionic poly(carboxybetaine) functionalized conducting polymer polyaniline nanowires for the electrochemical detection of carcinoembryonic antigen in undiluted blood serum. *Bioelectrochemistry* **125**, 90–96 (2019).

7. Antonietti, M., Hentze, H.-P., Smarsly, B., Löffler, M. & Morschhäuser, R. *Structure Characterization of Surfactant Assisted Polymer Thickeners by Silica Nanocasting*. *Macromol. Mater. Eng* vol. 287 (2002).

8. Wang, J., Wang, D. & Hui, N. A low fouling electrochemical biosensor based on the zwitterionic polypeptide doped conducting polymer PEDOT for breast cancer marker BRCA1 detection. *Bioelectrochemistry* **136**, (2020).

9. Wang, L. *et al.* Tough, Adhesive, Self-Healable, and Transparent Ionically Conductive Zwitterionic Nanocomposite Hydrogels as Skin Strain Sensors. *ACS Appl Mater Interfaces* **11**, 3506–3515 (2019).

10. Zeng, S. *et al.* Computer Simulations on a pH-Responsive Anticancer Drug Delivery System Using Zwitterion-Grafted Polyamidoamine Dendrimer Unimolecular Micelles. *Langmuir* **37**, 1225–1234 (2021).

11. Holm, C. *et al.* Polyelectrolyte Theory. *Advances in Polymer Science* vol. 166 67–111 Preprint at https://doi.org/10.1007/b11349 (2004).

12. Das, S., Eisen, A., Lin, Y. H. & Chan, H. S. A Lattice Model of Charge-Pattern-Dependent Polyampholyte Phase Separation. *Journal of Physical Chemistry B* vol. 122 5418–5431 Preprint at https://doi.org/10.1021/acs.jpcb.7b11723 (2018).

13. Yang, B. & Yuan, W. Highly Stretchable, Adhesive, and Mechanical Zwitterionic Nanocomposite Hydrogel Biomimetic Skin. *ACS Appl Mater Interfaces* (2019) doi:10.1021/acsami.9b14040.

14. Civera, M., Fornili, A., Sironi, M. & Fornili, S. L. *Molecular Dynamics Simulation of Aqueous Solutions of Glycine Betaine*. www.elsevier.com/locate/cplett.

15. Zheng, L., Sundaram, H. S., Wei, Z., Li, C. & Yuan, Z. Applications of zwitterionic polymers. *Reactive and Functional Polymers* vol. 118 51–61 Preprint at https://doi.org/10.1016/j.reactfunctpolym.2017.07.006 (2017).

16. Matsumura, K. & Hyon, S. H. Polyampholytes as low toxic efficient cryoprotective agents with antifreeze protein properties. *Biomaterials* **30**, 4842–4849 (2009).

17. Liu, M. *et al.* Dimethyl Sulfoxide-Free Cryopreservation of Chondrocytes Based on Zwitterionic Molecule and Polymers. *Biomacromolecules* **20**, 3980–3988 (2019).

18. Bernards, M. & He, Y. Polyampholyte polymers as a versatile zwitterionic biomaterial platform. *Journal of Biomaterials Science, Polymer Edition* vol. 25 1479–1488 Preprint at https://doi.org/10.1080/09205063.2014.938976 (2014).

19. Rajan, R. *et al.* Review of the current state of protein aggregation inhibition from a materials chemistry perspective: Special focus on polymeric materials. *Materials Advances* vol. 2 1139–1176 Preprint at https://doi.org/10.1039/d0ma00760a (2021).

20. Schulze, N., Appelhans, D., Tiersch, B. & Koetz, J. Morphological transformation of vesicles into tubular structures by adding polyampholytes or dendritic glycopolymers. *Colloids Surf A Physicochem Eng Asp* **457**, 326–332 (2014).

21. Higgs, P. G. & Joanny, J. F. Theory of polyampholyte solutions. *J Chem Phys* **94**, 1543–1554 (1991).

22. Zhang, Y., Liao, J., Wang, T., Sun, W. & Tong, Z. Polyampholyte Hydrogels with pH Modulated Shape Memory and Spontaneous Actuation. *Adv Funct Mater* **28**, (2018).

23. Tan, B. H., Ravi, P. & Tam, K. C. Synthesis and characterization of novel pH-responsive polyampholyte microgels. *Macromol Rapid Commun* **27**, 522–528 (2006).

24. Ogawa, K., Nakayama, A. & Kokufuta, E. Preparation and characterization of thermosensitive polyampholyte nanogels. *Langmuir* **19**, 3178–3184 (2003).

25. Kanazawa, R., Sasaki, A. & Tokuyama, H. Preparation of dual temperature/pH-sensitive polyampholyte gels and investigation of their protein adsorption behaviors. *Sep Purif Technol* **96**, 26–32 (2012).

26. Phan, Q. T. *et al.* Polyampholyte-grafted single walled carbon nanotubes prepared via a green process for anticancer drug delivery application. *Polymer (Guildf)* **193**, (2020).

27. Zurick, K. M. & Bernards, M. Recent biomedical advances with polyampholyte polymers. *Journal of Applied Polymer Science* vol. 131 Preprint at https://doi.org/10.1002/app.40069 (2014).

28. Matsumura, K., Bae, J. Y. & Hyon, S. H. Polyampholytes as cryoprotective agents for mammalian cell cryopreservation. *Cell Transplant* **19**, 691–699 (2010).

29. Feric, M. *et al.* Coexisting Liquid Phases Underlie Nucleolar Subcompartments. *Cell* **165**, 1686–1697 (2016).

30. Ianiro, A. *et al.* Liquid–liquid phase separation during amphiphilic self-assembly. *Nat Chem* **11**, 320–328 (2019).

31. Mohammadi, P. *et al.* Phase transitions as intermediate steps in the formation of molecularly engineered protein fibers. *Commun Biol* **1**, (2018).

32. Najafi, S. *et al.* Liquid–liquid phase separation of Tau by self and complex coacervation. *Protein Science* **30**, 1393–1407 (2021).

33. Hyman, A. A., Weber, C. A. & Jülicher, F. Liquid-liquid phase separation in biology. *Annual review of cell and developmental biology* vol. 30 39–58 Preprint at https://doi.org/10.1146/annurev-cellbio-100913-013325 (2014).

34. Aumiller, W. M. & Keating, C. D. Experimental models for dynamic compartmentalization of biomolecules in liquid organelles: Reversible formation and partitioning in aqueous biphasic systems. *Advances in Colloid and Interface Science* vol. 239 75–87 Preprint at https://doi.org/10.1016/j.cis.2016.06.011 (2017).

35. Lin, Y., Protter, D. S. W., Rosen, M. K. & Parker, R. Formation and Maturation of Phase-Separated Liquid Droplets by RNA-Binding Proteins. *Mol Cell* **60**, 208–219 (2015).

36. Molliex, A. *et al.* Phase Separation by Low Complexity Domains Promotes Stress Granule Assembly and Drives Pathological Fibrillization. *Cell* **163**, 123–133 (2015).

37. Pak, C. W. *et al.* Sequence Determinants of Intracellular Phase Separation by Complex Coacervation of a Disordered Protein. *Mol Cell* **63**, 72–85 (2016).

38. Brangwynne, C. P., Mitchison, T. J. & Hyman, A. A. Active liquid-like behavior of nucleoli determines their size and shape in Xenopus laevis oocytes. *Proc Natl Acad Sci U S A* **108**, 4334–4339 (2011).

39. Alberti, S. & Dormann, D. Liquid-Liquid Phase Separation in Disease. (2019) doi:10.1146/annurev-genet-112618.

40. Uversky, V. N. Intrinsically disordered proteins in overcrowded milieu: Membrane-less organelles, phase separation, and intrinsic disorder. *Current Opinion in Structural Biology* vol. 44 18–30 Preprint at https://doi.org/10.1016/j.sbi.2016.10.015 (2017).

41. Li, P. *et al.* Phase transitions in the assembly of multivalent signalling proteins. *Nature* **483**, 336–340 (2012).

42. Van Horn, W. D. *et al.* Solution nuclear magnetic resonance structure of membrane-integral diacylglycerol kinase. *Science (1979)* **324**, 1726–1729 (2009).

43. Kato, M. *et al.* Cell-free formation of RNA granules: Low complexity sequence domains form dynamic fibers within hydrogels. *Cell* **149**, 753–767 (2012).

44. Elbaum-Garfinkle, S. *et al.* The disordered P granule protein LAF-1 drives phase separation into droplets with tunable viscosity and dynamics. *Proc Natl Acad Sci U S A* **112**, 7189–7194 (2015).

45. Nott, T. J. *et al.* Phase Transition of a Disordered Nuage Protein Generates Environmentally Responsive Membraneless Organelles. *Mol Cell* **57**, 936–947 (2015).

46. Lee, S. & Kim, H.-J. Prion-like Mechanism in Amyotrophic Lateral Sclerosis: are Protein Aggregates the Key? *Exp Neurobiol* **24**, 1–7 (2015).

47. Ross, C. A. & Poirier, M. A. Protein aggregation and neurodegenerative disease. *Nat Med* **10**, S10 (2004).

48. McNaught, K. S. P. & Olanow, C. W. Protein aggregation in the pathogenesis of familial and sporadic Parkinson's disease. *Neurobiology of Aging* vol. 27 530–545 Preprint at https://doi.org/10.1016/j.neurobiolaging.2005.08.012 (2006).

49. Mata, I. F., Wedemeyer, W. J., Farrer, M. J., Taylor, J. P. & Gallo, K. A. LRRK2 in Parkinson's disease: protein domains and functional insights. *Trends in Neurosciences* vol. 29 286–293 Preprint at https://doi.org/10.1016/j.tins.2006.03.006 (2006).

50. Schmaljohann, D. Thermo- and pH-responsive polymers in drug delivery. *Advanced Drug Delivery Reviews* vol. 58 1655–1670 Preprint at https://doi.org/10.1016/j.addr.2006.09.020 (2006).

51. Wei, M., Gao, Y., Li, X. & Serpe, M. J. Stimuli-responsive polymers and their applications. *Polymer Chemistry* vol. 8 127–143 Preprint at https://doi.org/10.1039/c6py01585a (2017).

52. Sershen, S. R., Westcott, S. L., Halas, N. J. & West, J. L. *Temperature-Sensitive Polymer-Nanoshell Composites for Photothermally Modulated Drug Delivery*. *Young Investigator Award World Biomaterials Congress* (2000).

53. Li, M., He, X., Ling, Y. & Tang, H. Dual thermoresponsive homopolypeptide with LCST-type linkages and UCST-type pendants: Synthesis, characterization, and thermoresponsive properties. *Polymer (Guildf)* **132**, 264–272 (2017).

54. Taylor, M. J., Tomlins, P. & Sahota, T. S. Thermoresponsive gels. *Gels* vol. 3 Preprint at https://doi.org/10.3390/gels3010004 (2017).

55. Shimada, N. *et al.* Ureido-derivatized polymers based on both poly(allylurea) and poly(l -citrulline) exhibit UCST-type phase transition behavior under physiologically relevant conditions. *Biomacromolecules* **12**, 3418–3422 (2011).

56. Kuroyanagi, S. *et al.* Highly Ordered Polypeptide with UCST Phase Separation Behavior. *J Am Chem Soc* **141**, 1261–1268 (2019).

57. Schulz, D. N. *et al. Phase Behaviour and Solution Properties of Sulphobetaine Polymers*. (1986).

58. Tiwari, A. & Sancaktar, E. Poly(N-isopropylacrylamide) grafting solution parameters for controlling temperature responsiveness in PET membranes fabricated using 248 nm KrF excimer laser. *Eur Polym J* **103**, 220–227 (2018).

59. Okano, T., Yamada, N., Okuhara, M., Sakai, H. & Sakurai, Y. *Mechanism of Cell Detachment from Temperature-Modulated, Hydrophilic-Hydrophobic Polymer Surfaces*. *Biomateriols* vol. 16 (1995).

60. Plamper, F. A. *et al.* Tuning the thermoresponsive properties of weak poly electrolytes: Aqueous solutions of star-shaped and linear poly(N,N-dimethylaminoethyl methacrylate). *Macromolecules* **40**, 8361–8366 (2007).

61. Ebara, M. *et al.* Temperature-responsive cell culture surfaces enable 'on-off' affinity control between cell integrins and RGDS ligands. *Biomacromolecules* **5**, 505–510 (2004).

62. Halperin, A., Kröger, M. & Winnik, F. M. Poly(N -isopropylacrylamid)-Phasendiagramme: 50 Jahre Forschung . *Angewandte Chemie* **127**, 15558–15586 (2015).

63. Kushida, A. *et al. Decrease in Culture Temperature Releases Monolayer Endothelial Cell Sheets Together with Deposited Fibronectin Matrix from Temperature-Responsive Culture Surfaces*. (1999).

64. Akiyama, Y., Kikuchi, A., Yamato, M. & Okano, T. Ultrathin poly(N-isopropylacrylamide) grafted layer on polystyrene surfaces for cell adhesion/detachment control. *Langmuir* **20**, 5506–5511 (2004).

65. Dani, R. K., Schumann, C., Taratula, O. & Taratula, O. Temperature-tunable iron oxide nanoparticles for remote-controlled drug release. *AAPS PharmSciTech* **15**, 963–972 (2014).

66. Das, E. & Matsumura, K. Tunable phase-separation behavior of thermoresponsive polyampholytes through molecular design. *J Polym Sci A Polym Chem* **55**, 876–884 (2017).

67. Rajan, R., Pangkom, N. & Matsumura, K. Design of Stimuli-Responsive Polyampholytes and Their Transformation into Micro-Hydrogels for Drug Delivery. in *ACS Symposium Series* vol. 1350 47–62 (American Chemical Society, 2020).

68. Shi, C., He, Y., Feng, X. & Fu, D. ε-Polylysine and next-generation dendrigraft poly-L-lysine: Chemistry, activity, and applications in biopharmaceuticals. *J Biomater Sci Polym Ed* **26**, 1343–1356 (2015).

69. Tacar, O., Sriamornsak, P. & Dass, C. R. Doxorubicin: An update on anticancer molecular action, toxicity and novel drug delivery systems. *Journal of Pharmacy and Pharmacology* vol. 65 157–170 Preprint at https://doi.org/10.1111/j.2042-7158.2012.01567.x (2013).

70. Pridgen, E. M., Alexis, F. & Farokhzad, O. C. Polymeric nanoparticle drug delivery technologies for oral delivery applications. *Expert Opinion on Drug Delivery* vol. 12 1459–1473 Preprint at https://doi.org/10.1517/17425247.2015.1018175 (2015).

71. Tiwari, G. *et al.* Drug delivery systems: An updated review. *Int J Pharm Investig* **2**, 2 (2012).

72. Siepmann, J. & Siepmann, F. Mathematical modeling of drug delivery. *International Journal of Pharmaceutics* vol. 364 328–343 Preprint at https://doi.org/10.1016/j.ijpharm.2008.09.004 (2008).

73. Jain, K., Vedarajan, R., Watanabe, M., Ishikiriyama, M. & Matsumi, N. Tunable LCST behavior of poly(N-isopropylacrylamide/ionic liquid) copolymers. *Polym Chem* **6**, 6819–6825 (2015).

74. Khan, M. S. *et al.* Unravelling the potential of mitochondria-targeted liposomes for enhanced cancer treatment. *Drug Discovery Today* vol. 29 Preprint at https://doi.org/10.1016/j.drudis.2023.103819 (2024).

75. Hara, T., Iriyama, S., Makino, K., Terada, H. & Ohya, M. Mathematical description of drug movement into tumor with EPR effect and estimation of its configuration for DDS. *Colloids Surf B Biointerfaces* **75**, 42–46 (2010).

76. Orellana-Tavra, C., Köppen, M., Li, A., Stock, N. & Fairen-Jimenez, D. Biocompatible, Crystalline, and Amorphous Bismuth-Based Metal-Organic Frameworks for Drug Delivery. *ACS Appl Mater Interfaces* **12**, 5633–5641 (2020).

77. Aoki, K. & Saito, N. Biodegradable polymers as drug delivery systems for bone regeneration. *Pharmaceutics* vol. 12 Preprint at https://doi.org/10.3390/pharmaceutics12020095 (2020).

78. Liang, J., Peng, X., Zhou, X., Zou, J. & Cheng, L. Emerging applications of drug delivery systems in oral infectious diseases prevention and treatment. *Molecules* vol. 25 Preprint at https://doi.org/10.3390/molecules25030516 (2020).

79. Daraee, H. *et al.* Application of gold nanoparticles in biomedical and drug delivery. *Artificial Cells, Nanomedicine and Biotechnology* vol. 44 410–422 Preprint at https://doi.org/10.3109/21691401.2014.955107 (2016).

80. Lee, J., Chatterjee, D. K., Lee, M. H. & Krishnan, S. Gold nanoparticles in breast cancer treatment: Promise and potential pitfalls. *Cancer Letters* vol. 347 46–53 Preprint at https://doi.org/10.1016/j.canlet.2014.02.006 (2014).

81. Chechetka, S. A. *et al.* Light-driven liquid metal nanotransformers for biomedical theranostics. *Nat Commun* **8**, (2017).

82. Yan, J. *et al.* Fabrication of a pH/Redox-Triggered Mesoporous Silica-Based Nanoparticle with Microfluidics for Anticancer Drugs Doxorubicin and Paclitaxel Codelivery. *ACS Appl Bio Mater* **3**, 1216–1225 (2020).

83. Sebeke, L. C. *et al.* Hyperthermia-induced doxorubicin delivery from thermosensitive liposomes via MR-HIFU in a pig model. *Journal of Controlled Release* **343**, 798–812 (2022).

84. Needham, D. & Dewhirst, M. W. *The Development and Testing of a New Temperature-Sensitive Drug Delivery System for the Treatment of Solid*

Tumors. *Advanced Drug Delivery Reviews* vol. 53 www.elsevier.com/locate/drugdeliv (2001).

85. Sardar, R., Funston, A. M., Mulvaney, P. & Murray, R. W. Gold nanoparticles: Past, present, and future. *Langmuir* **25**, 13840–13851 (2009).

86. Sztandera, K., Gorzkiewicz, ;, Klajnert-Maculewicz, B. & Gorzkiewicz, M. *Gold Nanoparticles in Cancer Treatment*. http://pubs.acs.org (2018).

87. Lu, Y. *et al.* Transformable liquid-metal nanomedicine. *Nat Commun* **6**, (2015).

88. Ma, J. *et al.* Liquid Metal Nanoparticles as Initiators for Radical Polymerization of Vinyl Monomers. *ACS Macro Lett* **8**, 1522–1527 (2019).

Chapter 2

Elucidation of the liquid-liquid phase separation mechanism of Polyampholytes

2-1 Introduction

As mentioned in Chapter 1, liquid-liquid phase separation behavior is intricately related to various biological functions including metabolism in living organisms, and analyzing what strongly affects the behavior is important for phase separation. It has the potential to become the key to understanding life from a biological perspective and new treatments for diseases[1-6]. Since a wide variety of proteins already exist, it is expected that new compounds exhibiting LLPS behavior[3, 4] will continue to be synthesized and increase in number.

Since the properties of ampholyte polymers, which are also model compounds for proteins, change depending on the combination of acidic and basic groups, it can be assumed that countless types of ampholyte polymers will be synthesized and researched[7]. In addition, not only from the perspective of phase separation biology, but also because ampholyte polymers have high biocompatibility and responsiveness to external stimuli, they have the potential to be applied to biomaterials as intelligent materials[8-10]. One of the important points when applying materials as intelligent materials is how precisely their properties can be controlled[11]. The precision of polymer synthesis is also an effective factor in controlling properties, but the presence or absence of basic research on what strongly causes these properties has a wide impact, from the design of the polymer to the setting of the application environment[12].

In general, when properties are acquired through structural changes such as phase transitions, it is not due to only one effect, but it can be said that interactions with other properties of the polymer also have an influence[13]. Therefore, even if they have similar structures, their properties may change significantly by modifying a part of them. PNIPAM, which was mentioned in Chapter 1, is one of them, and its phase separation temperature changes significantly by modifying part of its structure or increasing its molecular weight[14, 15]. The same is true for ampholyte polymers, and

it can be said that it is necessary to study the mechanism for each compound that exhibits LLPS behavior.

Currently, the experimental and measurement methods necessary to study the mechanism of liquid-liquid phase separation behavior have not yet been established. This is also related to the fact that, as mentioned earlier, there is a strong possibility that the mechanisms differ for each compound that exhibits LLPS. Therefore, in this chapter, I focused on the droplet generation stage, which is the first stage in which LLPS is triggered, and performed multi-scale measurements. Phase separation behavior was evaluated by measuring on a scale from the occurrence of LLPS behavior to droplet formation. The ampholyte polymers used were PLL-SA, which was used in previous research, and carboxylated phthalic anhydride polylysine (PLL-PA). PLL-PA is a product in which a benzene ring is introduced for stabilization through hydrophobic interaction in order to overcome the problem that phase separation behavior is resolved when inhibited by salts present in the solvent of PLL-SA. Both are compounds having an amino group as an acidic group and a carboxyl group as a basic group, and have the same degree of polymerization. I evaluated by comparing and measuring how the introduction of a hydrophobic site caused a difference in the initial stage of phase separation.

2-2 Experiment

2-2-1 Materials

A 25% ε-polylysine solution was procured from JNC Corporation (Tokyo, Japan). Anhydrous succinic acid and anhydrous phthalic acid were obtained from Nacalai Tesque Inc. (Kyoto, Japan). The powder form of phosphate-buffered saline (PBS (-)) was purchased from Shimadzu Diagnostics Corp. (Tokyo, Japan).

2-2-2 Preparation of temperature responsive polyampholytes

An aqueous solution of 25% PLL was prepared, and an appropriate amount of SA or PA was added to the solution. The mixture was stirred at 60°C until complete dissolution of reagents. Fifty per cent of the amino groups of PLL carboxylated with SA or PA, were denoted as PLL-SA50 and PLL-PA50, respectively. The polymer solution obtained was lyophilised and stored in vacuum until usage. Sample solutions were prepared in arbitrary solvents and concentrations for the various measurements.

2-3 Characterization

For various measurements, PLL-SA50 and PLL-PA50 and polymers containing equal amounts of acidic and basic groups were used.

In USAXS/SAXS measurements, DLS measurements, and observations using a scanning laser microscope, PLL-SA50 and PLL-PA50 were prepared in an aqueous solution with the concentration adjusted so that the phase separation temperature was as close as possible to 33-35°C. For comparison purposes, an aqueous solution sample and a PBS solution sample with the

same polymer concentration were also prepared and measured. A table listing sample conditions is shown in Table 1.

Table 1 Sample conditions used for measurement

solvent	water		PBS	
Polymer	PLL-PA50	PLL-SA50	PLL-PA50	PLL-SA50
Tc(℃)	35	33	47	
Concentration(wt/v%)	19	40	19	40

In neutron scattering measurements, the polymer concentration was fixed at 20 w/v% and adjusted using three types of solvents: pure water solvent (H_2O), mixed solvent of heavy water and pure water (M_2O), and heavy water solvent (D_2O).

2-3-1 UV-Vis spectrophotometer

The temperature responsiveness and phase separation temperature were determined using a temperature-controlled UV-Vis spectrophotometer (UV-1800, Shimadzu Corp., Kyoto, Japan). Polymer solutions were placed in 2 mL quartz cells, and optical data were collected continuously at a fixed wavelength of 550 nm, while varying the temperature. The transmitted light intensity of the homogeneous solution state prior to phase separation was set as 100%, and the temperature at which the transmitted light intensity reached 50% was defined as the phase separation temperature.

The Tc of the sample solutions used in the following characteristic evaluations was measured and adjusted in the same manner.

2-3-2 Laser scanning microscope

Using a heated slide glass (Figure 9b) with a scanning laser microscope (LaSCOPE LM9001 manufactured by Astrodesign) (Figure 9a), the process of solution/droplet formation before and after phase separation was observed at elevated temperatures.

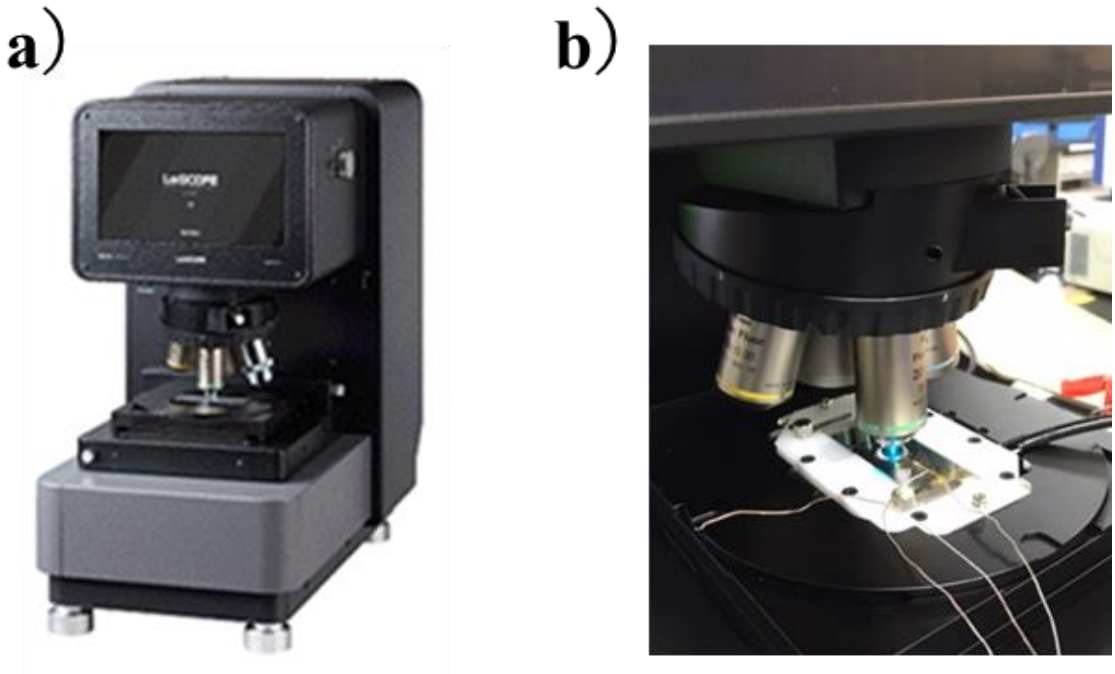

Figure 9 Scanning laser microscope used for observation (a)/heated slide glass (b)

2-3-3 Dynamic Light Scattering (DLS) Measurements

The DLS measurements analyzed the dynamics of the solution. Our goal was to evaluate the droplet formation and growth range, which is larger than the range that can be measured by neutron scattering or USAXS/SAXS.

2-3-4 Ultra-Small-Angle/Small-Angle X-ray Scattering (USAXS/SAXS) measurements

The measurements were performed using the BL08B2 equipment at Spring-8[16, 17], and the results were analyzed and evaluated. It has a temperature range of 100-1100K, and in this measurement, the temperature was raised from 10℃ to 60℃.

2-3-5 Neutron scattering measurement

I used the BL-21 high-intensity total scattering apparatus (NOVA) located at J-Parc[18, 19]. (Figure10) NOVA has a wide Q range. Here, I conducted measurements to measure the interactions and fluctuations between the polymer and solution before droplet formation. In addition to different solvents, the samples were filled with two types: a homogeneous solution before phase separation and a concentrated phase after phase separation, and measurements were taken while increasing the temperature.

Figure10　NOVA sample insertion port used for measurement and image of the measured sample

2-4 Results and discussion

2-4-1 Synthesis of temperature-responsive polyampholytes

Temperature-responsive polyampholytes, PLL-SA and PLL-PA, were synthesised by adding SA and PA to a PLL solution, according to Scheme 1.

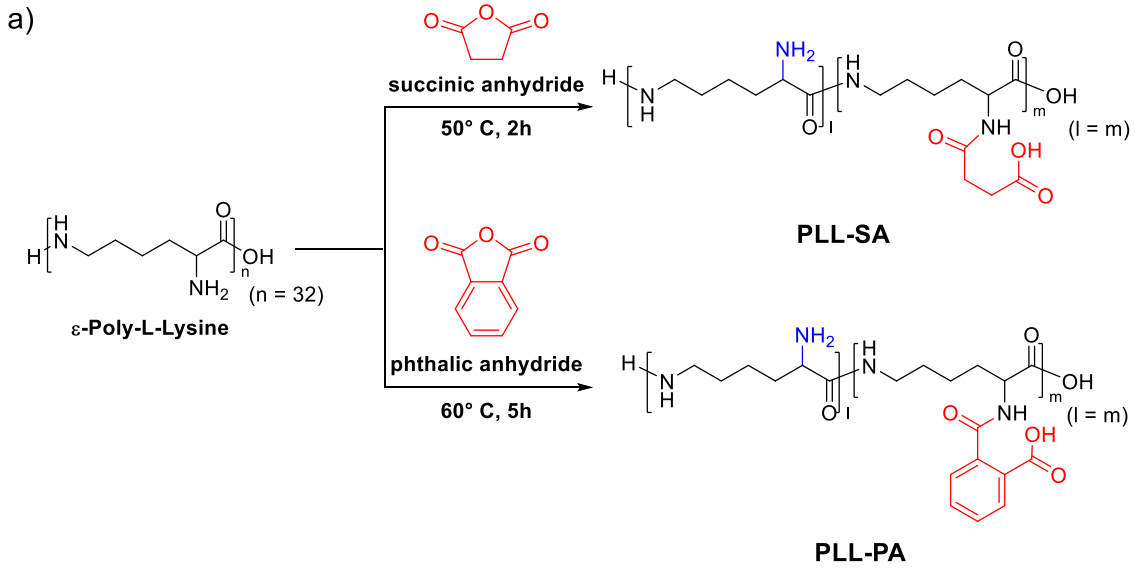

Scheme 1Synthesis of PLL-SA and PLL-PA

The synthesis was performed under heating and stirring conditions, resulting in the formation of carboxylated polylysine solutions. Degree of substitution was calculated from integration values using ^{1}H NMR spectroscopy and utilizing the following equation. (Figure 11 and Table 2)

$$PA(\%) = \frac{\frac{[a,b,c,d]}{4}}{\frac{\delta}{4} + \frac{[a,b,c,d]}{4}} \times 100$$

Table2 Characterization of polyampholytes

	composition (in feed)		composition (NMR)	
	NH_2	COOH	NH_2	COOH
PLL	100	0	100	0
PLL-PA50	50	50	49	51

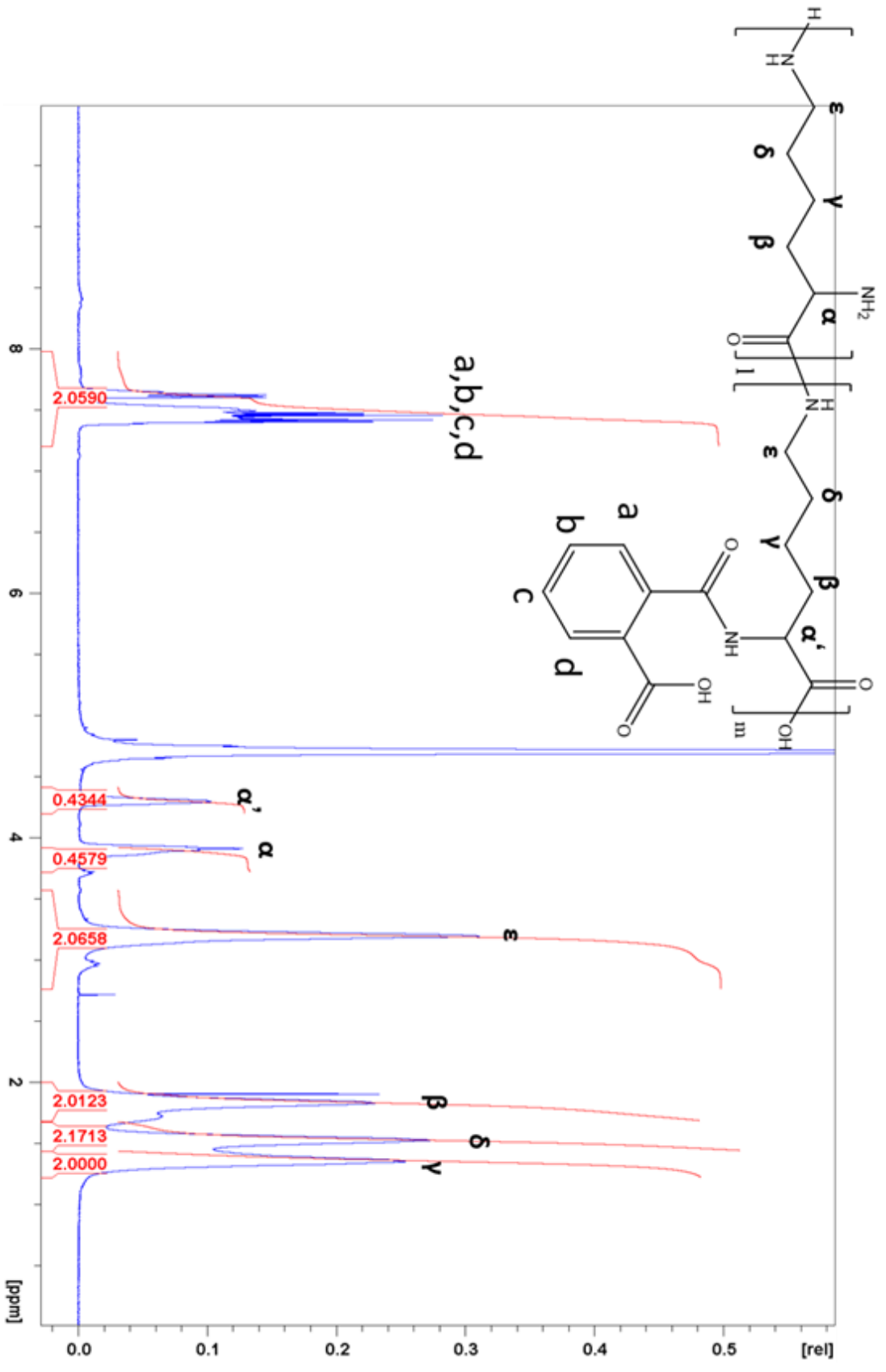

Figure 11 ^{1}H-NMR of PLL-PA50(solvent : D_2O)

2-4-2 UV-Vis spectrophotometer

To assess the temperature responsiveness of PLL-PA in both pure water and saline solution, I conducted measurements of transmitted light intensity using a temperature-variable UV-Vis spectrophotometer. In case of PLL-SA50, phase separation was observed only in pure aqueous solution, as shown in Figure 12(A); the phase separation temperatures for different concentrations of PLL-SA50 in pure water solvent were as follows: 3.2, 11 and 41°C at 12, 12.5 and 15% transmittances, respectively. No change in the transmitted light intensity was observed at any concentration with PBS as solvent. The phase separation temperatures at 12% and 15% polymer concentrations were 3.2°C and 41°C, respectively, indicating that phase separation can be induced over a wide range of temperatures by adjusting polymer concentration. In contrast, phase separation temperatures for different polymer concentrations of PLL-PA50 in pure water solvent were as follows: 11.5, 19 and 34°C at 22.5, 25 and 30% transmittances, respectively. In PBS solvent, the temperatures were 27.5, 37 and 50°C at 20, 25, 30% transmittances, respectively. PLL-PA exhibited phase separation in aqueous solution and PBS (Figure 12（B)）, suggesting that PLL-PA can be used over a wide temperature range by adjusting polymer concentration in the physiological salt environment. The phase separation temperature curves obtained from these experiments confirm the presence of LCST-type phase separation and demonstrate that the phase separation temperature can be tuned over a wide range by adjusting polymer concentration.

This measurement enables the evaluation of both temperature responsiveness and the behavior of liquid-liquid phase separation. It is established that the range of liquid-liquid phase separation behavior measurable through transmitted light is 1 nm or greater[20]. Generally, the particle sizes at which transparency decreases are observed to be 1 nm or greater, with size of 100 nm or more resulting in pronounced cloudiness. In this study, the temperature at which the intensity of transmitted light intensity reduces to 50% is defined as the phase separation temperature. On a

macroscopic level, the behavior of separation becomes visually discernible as the solution turns cloudy and separates into two distinct phases. Nevertheless, the determination of transparency is inherently qualitative, necessitating the need for quantitative evidence for rigorous analysis. Therefore, the measurement of transmitted light intensity emerges as a critical method for acquiring quantitative data on the behavior of liquid-liquid phase separation.

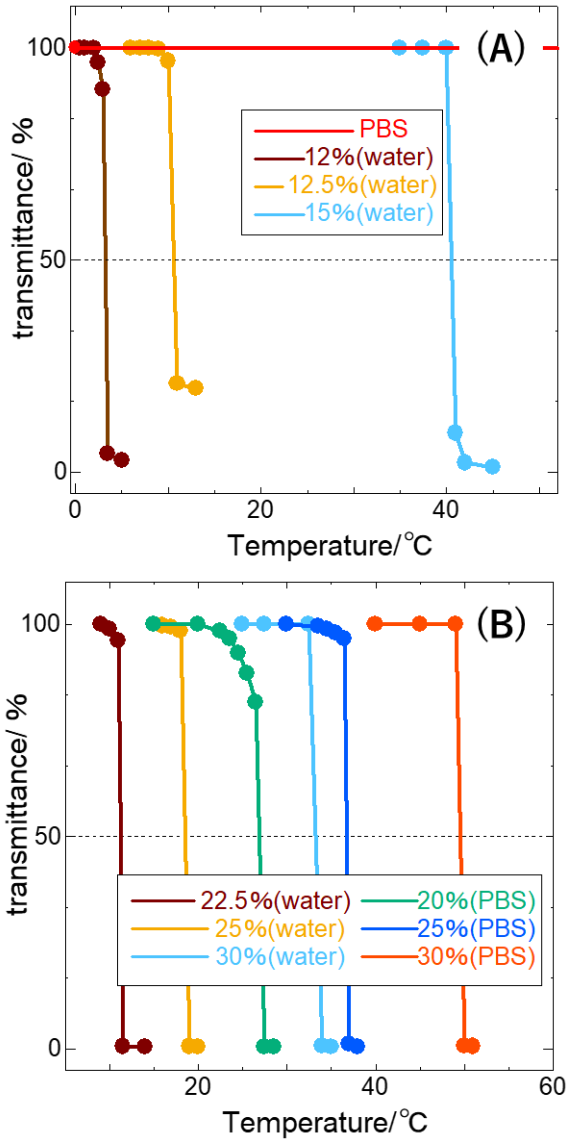

Figure 12 Changes in Transmittance Intensity Across Different Temperature Ranges (UV-vis, λ=550nm; 50% Transmittance Indicates Phase Separation Temperature) (A) The phase separation temperatures for different polymer concentrations of PLL-SA50 in pure water (B) The phase separation temperatures for different polymer concentrations of PLL-PA50 in pure water and PBS

Generally, the particle sizes at which transparency decreases are observed to be 1 nm or greater, with size of 100 nm or more resulting in pronounced cloudiness[21]. In this study, the temperature at which the intensity of transmitted light intensity reduces to 50% is defined as the phase separation temperature. On a macroscopic level, the behavior of separation becomes visually discernible as the solution turns cloudy and separates into two distinct phases. Nevertheless, the determination of transparency is inherently qualitative, necessitating the need for quantitative evidence for rigorous analysis. Therefore, the measurement of transmitted light intensity emerges as a critical method for acquiring quantitative data on the behavior of liquid-liquid phase separation.

2-4-3 Laser scanning microscope

The video demonstrates the droplet formation process in PLL-SA water solvent and PLL-PA water/PBS solvent near the phase separation temperature captured during heating observation using a scanning laser microscope (Figure 13). As mentioned above, the presence of PBS solvent for PLL-SA suppresses phase separation behavior due to salt interface, resulting in the absence of observable droplet formation. Droplet formation and growth were observed in all samples that exhibited phase separation behavior due to temperature increase. In PLL-SA, fine droplets of irregular size were continuously formed and subsequently aggregated, whereas in PLL-PA system, droplets of somewhat uniform size were rapidly formed and then enlarged. The rate of coalescence of droplets in the PLL-PA was also slower than that of PLL-SA, indicating enhanced stability of PLL-PA during the droplet growth stage.

It is already known that the phase separation behavior of PLL-SA is caused by the electrostatic interactions between amino groups and carboxy groups[22]. The newly synthesized PLL-PA , despite having the same ratios of these functional groups and a molecular weight difference of

approximately 770, exhibits distinct phase separation behavior in the physiological salt solution. This divergence is likely attributable to π-π interactions facilitated by the aromatic ring introduced in the PLL-PA structure, particularly in the presence of salt solvents[22-24]. Such interactions are not prevalent in the PLL-SA system, highlighting the critical role of molecular structure and specific intermolecular forces in dictating phase separation dynamics.

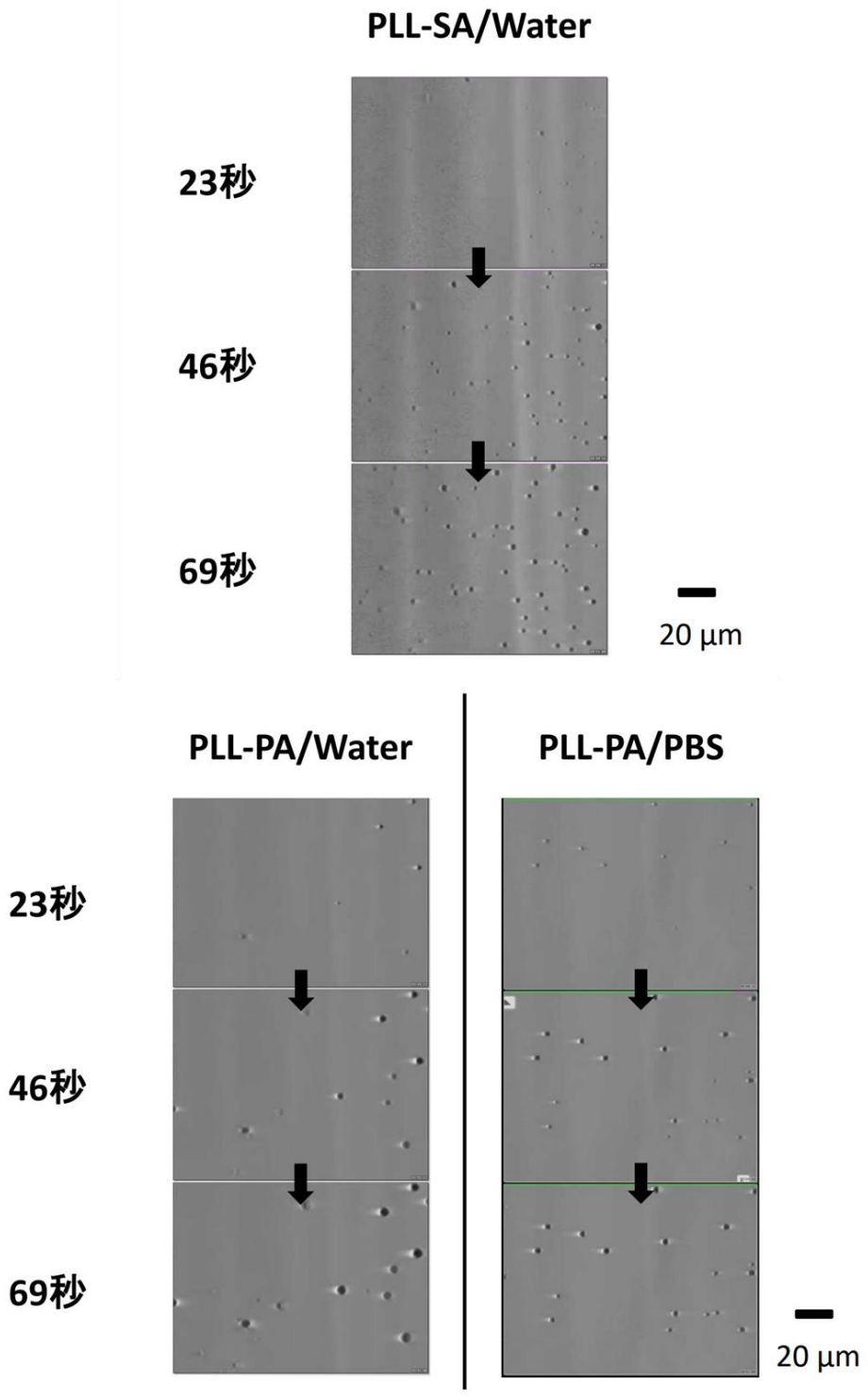

Figure 13　Captured image of the heating process of a polymer solution using a scanning laser

2-4-4 Dynamic Light Scattering (DLS) Measurements

In my investigation of droplet formation dynamics, DLS measurements provided insight into the changes at a finer scale than could be observed by laser microscopy. The DLS measurement results are shown in Figure 14.

Excluding the PLL-SA/PBS system, where phase separation behavior is suppressed, a notable variation in the autocorrelation coefficient with increasing temperature was observed. It can be confirmed that the PLL-SA system changes continuously with temperature increasing regardless of the phase separation temperature. In contrast, in the PLL-PA system, significant changes in the autocorrelation coefficient were observed beyond the phase separation temperature. This distinction aligns with the previously noted behavior where PLL-SA exhibits continuous formation of unstable and small-sized droplets, whereas PLL-PA is characterized by the rapid formation of droplets of a relatively uniform size.

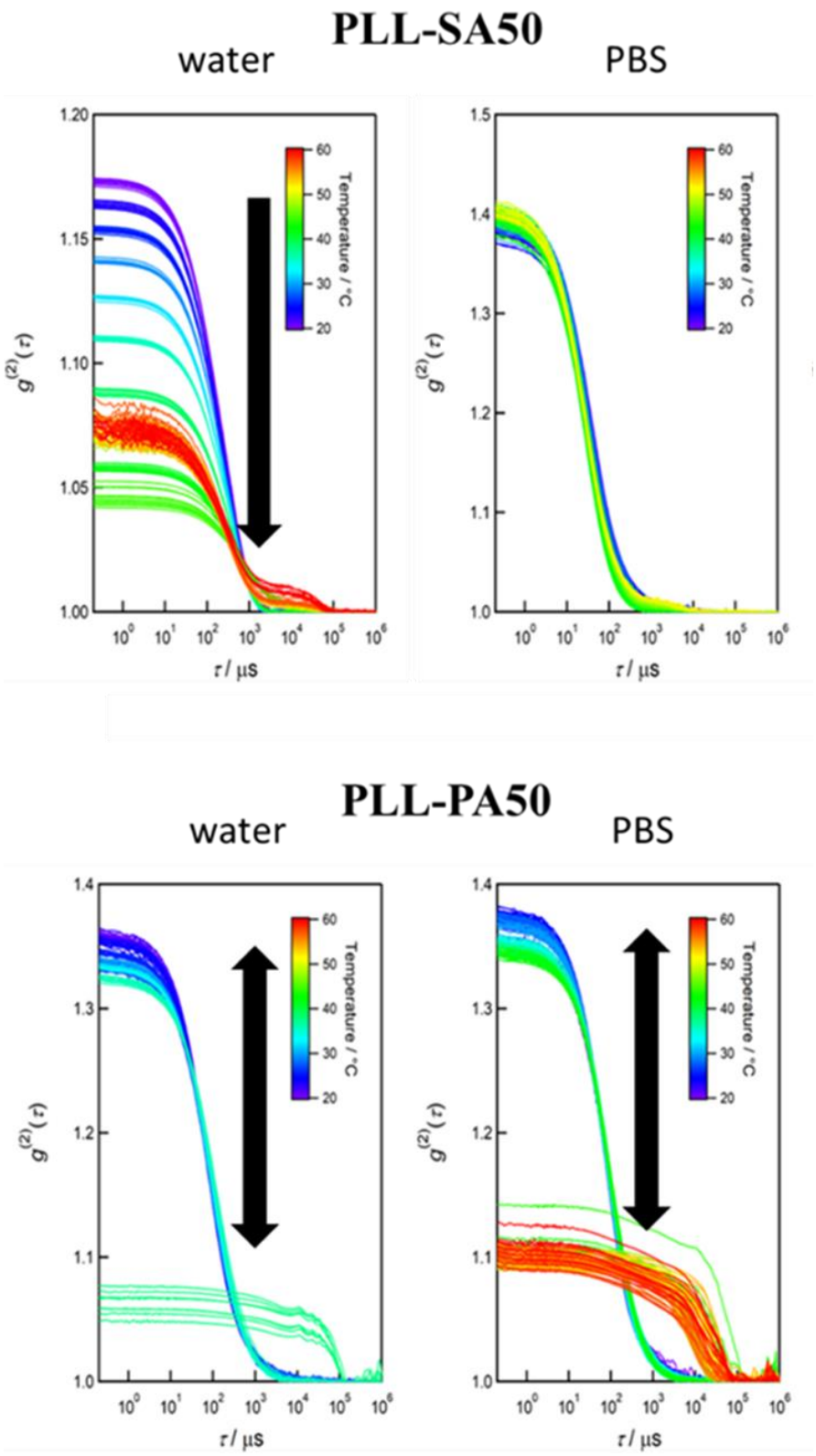

Figure 14 Autocorrelation coefficient and temperature dependence

Although the precise minimum diameters of droplets formed by PLL-SA and PLL-PA remain undetermined, it is hypothesized that they are akin to proteins with analogous properties, which these compounds model. Given that vesicle sizes within biological cells span from several hundred nanometers to a few micrometers[25-27], the observed continuous decrease in the autocorrelation coefficient for PLL-SA prior to reaching the phase separation temperature may not necessarily indicate droplet formation[28]. Instead, this trend could suggest fluctuations occurring in advance of droplet emergence[29]. This phenomenon was not evident in the PLL-PA system, hinting at the possibility that, despite superficially similar phase separation behaviors at the macroscopic level, the underlying mechanisms may differ significantly.

The observation that the autocorrelation coefficient does not drop to zero but stabilizes at a low value beyond the phase separation temperature is attributed to measurements being conducted in regions where droplets were actively growing and undergoing coacervation. This persistence of a non-zero autocorrelation coefficient underscores the dynamic nature of droplet formation and growth, reflecting continuous structural changes at the microscopic scale.

2-4-5 Ultra-Small-Angle/Small-Angle X-ray Scattering (USAXS/SAXS) measurements

In order to investigate the phase separation behavior at a more detailed scale, USAXS/SAXS measurements were performed using a similar sample. The data obtained by the measurements are shown below. (Figure 15)

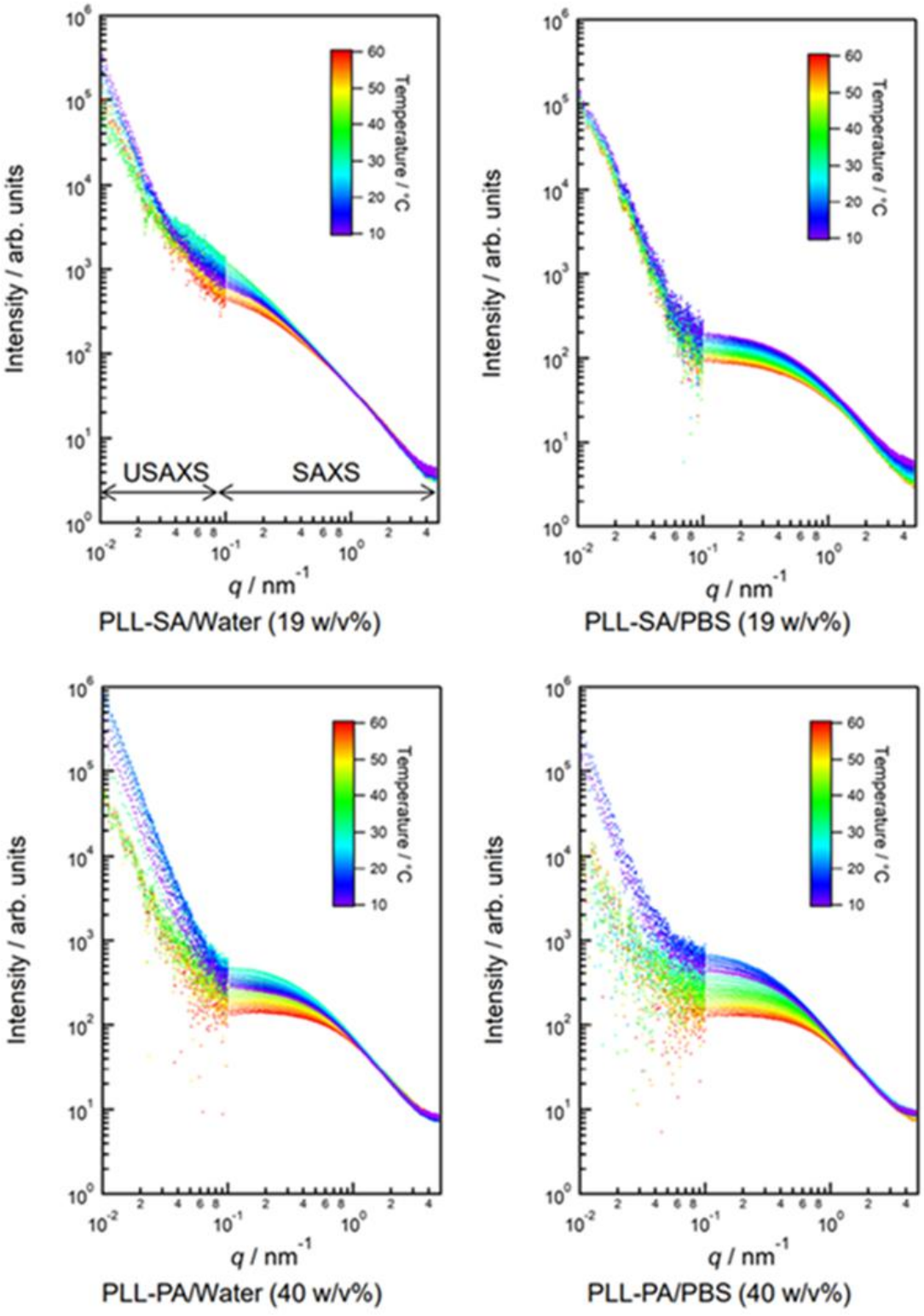

Figure 15 USAXS/SAXS measurement results

After confirming that both USAX/SAXS measurements were capable of resolving structures on the nanometer scale, I proceed to analyze the relationship between correlation length and temperature as well as relaxation time and temperature. The analysis results are shown in Figure 16. Analysis was performed using the Olstein-Zernike equation[30, 31] in the USAX measurement region and the Debye-Bueche equation[32, 33] in the SAXS region. The following formula was used for this fitting.

$$I(Q) = \frac{I_{\mathrm{DB}}}{(1 + \xi_{DB}^2 Q^2)^2} + \frac{I_{OZ}}{1 + \xi_{\mathrm{OZ}}^2 Q^2} + BG$$

I(Q): scattering intensity

I_{DB}: intensity of the Debye-Bueche component

ξ_{DB}: correlation length of the Debye-Bueche component

I_{OZ}: stands for the intensity of the Ornstein-Zernike component

ξ_{OZ}: correlation length of the Ornstein-Zernike component

BG" corresponds to the scattering background.

In the high-q region ($q > 10^{-2}$ Å^{-1}), the scattering intensity decays with q and converges to a temperature-independent curve. This phenomenon highlights the diminishing influence of thermal fluctuations on scattering at smaller length scales. In the mid-q region (10^{-3} Å$<q<10^{-2}$ Å^{-1}) a plateau in scattering intensity is observed, which becomes more pronounced with decreasing temperature. This plateau indicates enhanced concentration fluctuations within a homogeneous state, directly linked to the thermal conditions of the system. In the low-q region ($q < 10^{-3}$ Å^{-1}) the scattering intensity becomes independent of temperature again , suggesting a return to uniformity over larger scales. This observation underscores the scale-dependent nature of scattering phenomena. The Ornstein-Zernike equation is adept at describing scattering from concentration fluctuations in both the intermediate and high q regions[34, 35], offering a theoretical framework for

understanding the observed patterns. Conversely, in the low q region, where scattering is influenced by random non-uniformities, the Debye-Bueche equation provides a more accurate description. By integrating the Ornstein-Zernike and Debye-Bueche equations, a comprehensive model can be developed to fit the scattering characteristics across the entire range of q values. This approach allows for a unified understanding of scattering behavior, highlighting the interplay between thermal fluctuations, concentration variations, and structural non-uniformities.

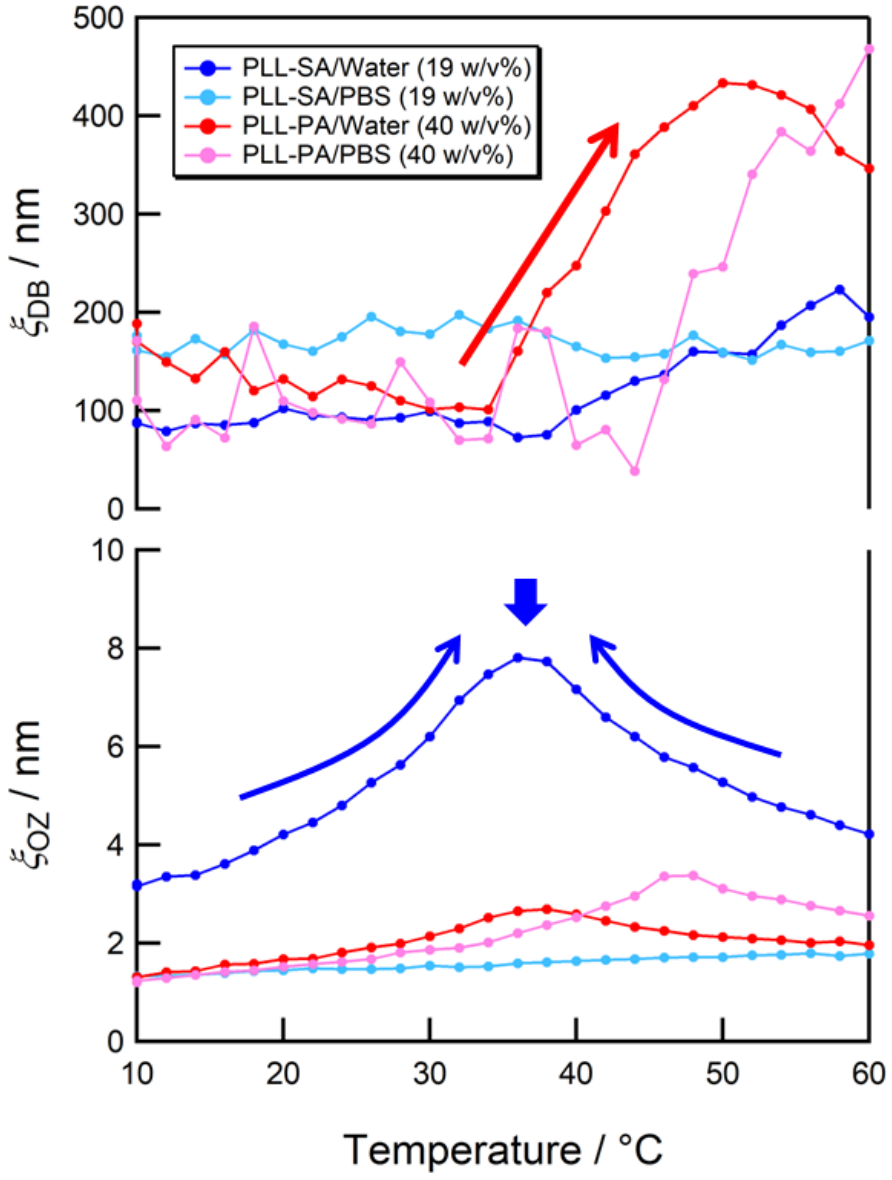

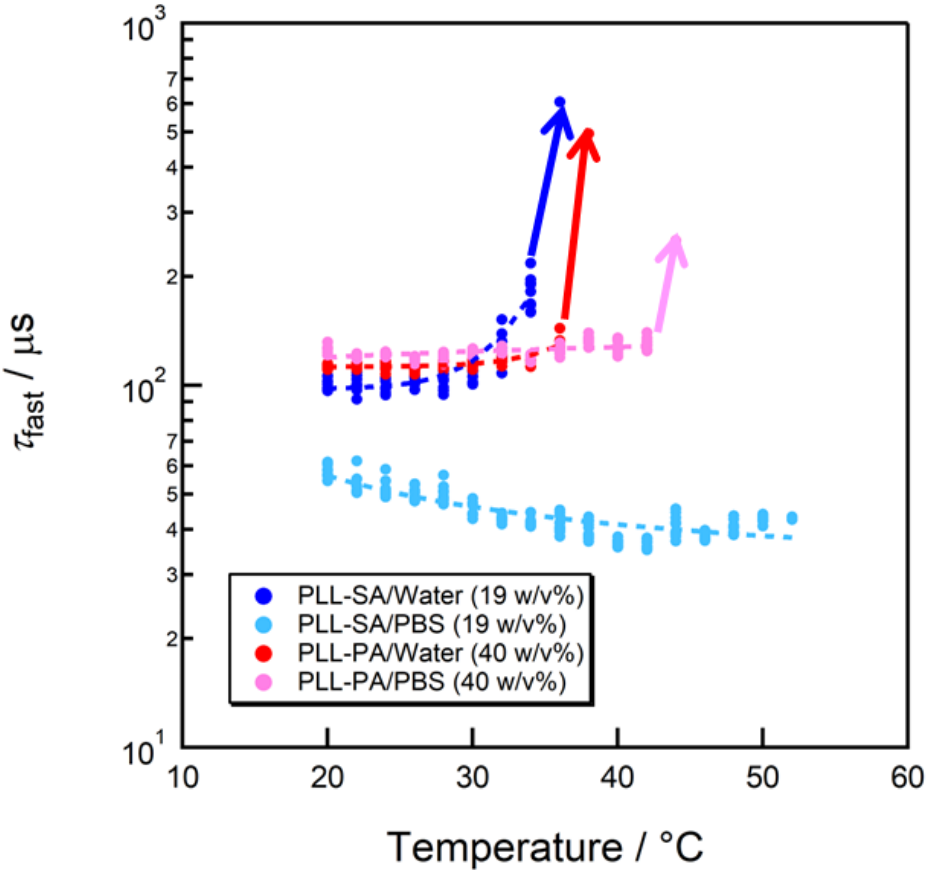

Figure 16 Analysis results regarding temperature of correlation length and relaxation time

The concept of correlation length is pivotal for elucidating changes in the phases of substances, including phase transitions and critical phenomena. It is defined as the distance over which the correlation function decreases to a certain value, serving as a measure of the extent to which particles or phases are correlated with each other across distance[36-38].

A smaller correlation length suggests that order within the system is localized, indicating that the likelihood of observing critical phenomena is reduced. Conversely, a divergence in the correlation length signifies that the system is nearing a critical point, heralding an imminent phase transition. This behavior underscores the correlation length's role in predicting the system's approach to criticality and its transition from one phase to another.

2-4-6 Neutron scattering measurement

Neutron scattering experiments were conducted to investigate the dynamics of polymer solutions and their interaction with water based on a series of trends. PLL-SA50 and PLL-PA50 were prepared using three types of solvents: pure water, a mixed solvent of pure water and heavy water, and heavy water. The experimental setup aimed to leverage the contrasting neutron scattering lengths of hydrogen and deuterium to differentiate the polymer-solvent interactions under varying hydration levels and solvent compositions. Sample identifiers, used to distinguish between the different solution conditions, are provided adjacent to Figure 17 for reference.

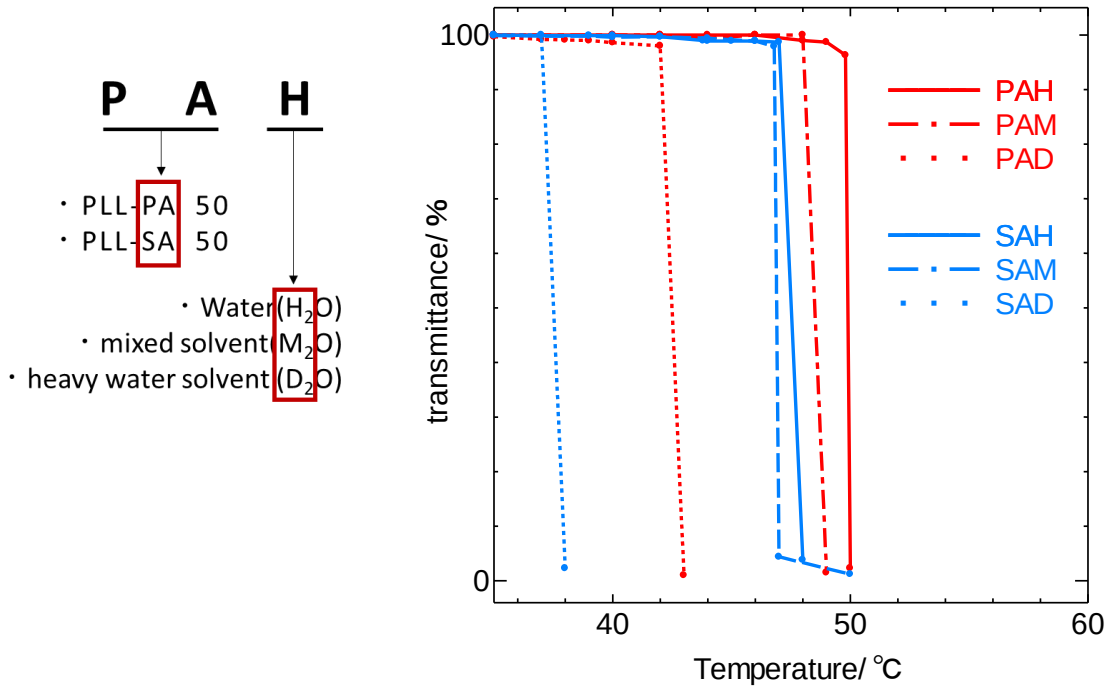

Figure17 Sample label and phase separation temperature used for neutron scattering measurements

To ensure comparability across experiments, the concentration of the polymers were adjusted to normalize the phase separation temperature when dissolved in pure water. PLL-SA50 was prepared at a concentration of 20wt/v%, resulting in phase separation temperature of 47.9℃, while PLL-PA50 was set at 40wt/v%, achieving a phase separation temperature of 49.9℃. Similar polymer concentrations were utilized for samples involving intermediate mixtures of water and heavy water, facilitating a direct comparison across solvent systems. Measurements of transmitted light intensity, as depicted in Figure 17, indicate a notable decrease in phase separation temperature with an increased proportion of heavy water, despite the uniform polymer concentration. This phenomenon, consistently observed in both PLL-SA and PLL-PA samples, is attributed to the distinct density differences between heavy water and pure water, which presumably affect the phase behavior of the polymer solutions. To enhance the precision of our data, initial measurements were conducted at a fixed temperature of 300K, below the phase separation threshold, with a heightened number of integrations for accuracy. The fortuitous availability of additional machine time permitted further exploration of phase behavior in heavy water solutions. Specifically, SAD and PAD measurements were carried out at 35°C and 50°C for one hour each, alongside detailed PAD analyses conducted at 1°C increments ranging from 39°C to 44°C, each for a duration of one hour. The outcomes of these meticulous measurements are presented in Figure 18.

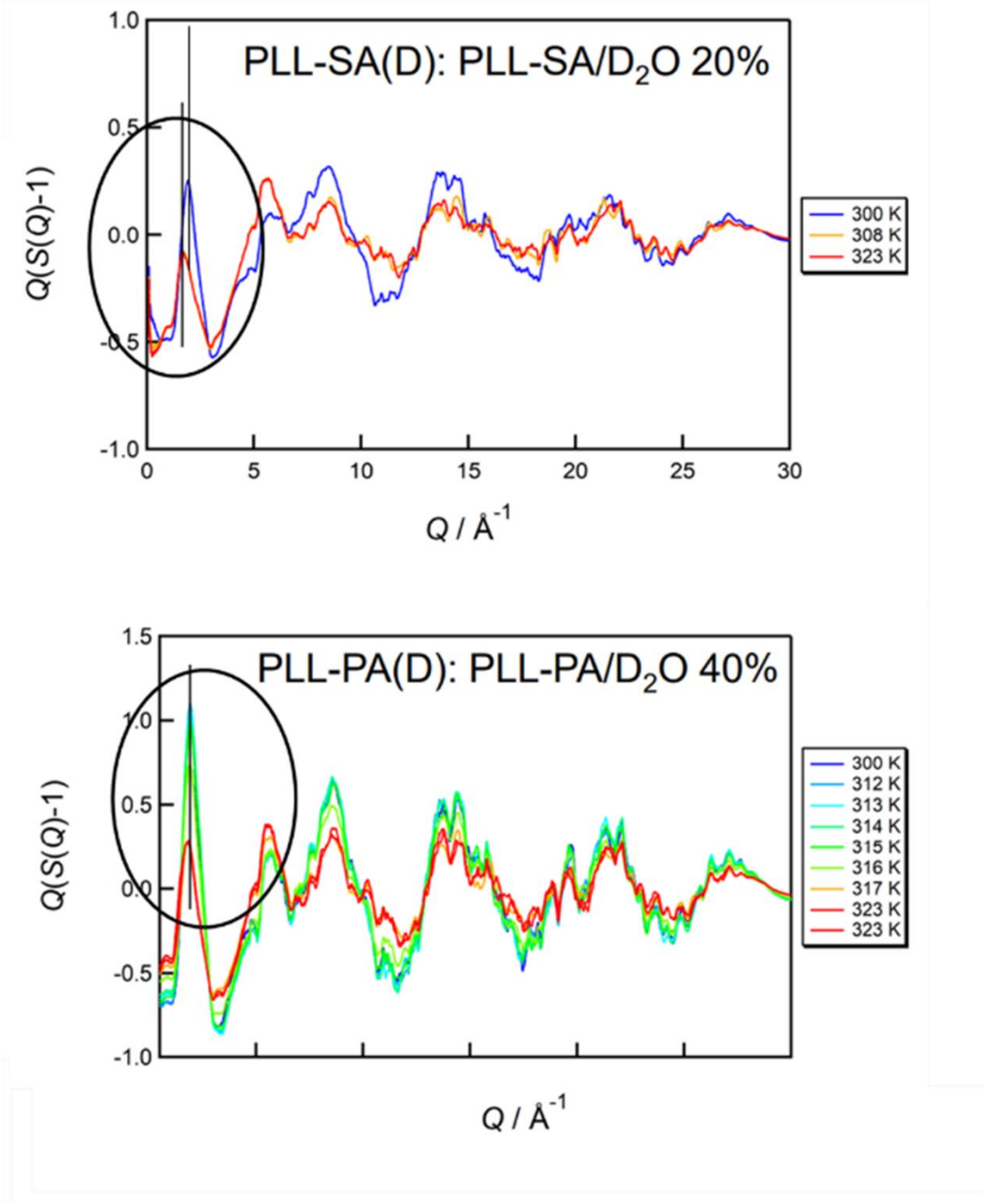

Figure18 Neutron scattering measurement results for 1 hour in temperature range

Alterations in the structural factors of the hydrated sections were specifically noted in SAD before and subsequent to phase separation. Initial analysis across various scales suggested the presence of a consistent trend. However, the requisite adjustment of polymer concentrations to equalize phase separation temperatures introduced a significant variation that complicates straightforward comparison and discussion of these observations. Therefore, it was concluded that a direct comparison of the results, within the framework of this measurement approach, is not feasible.

2-5 Conclusion

This chapter delves into the study of two types of polymers: PLL-SA, which is a temperature-responsive ampholyte polymer that exhibits liquid-liquid phase separation behavior, and PLL-PA, which has a hydrophobic moiety introduced into the PLL-SA structure. The phase separation behavior was compared and discussed. It was confirmed that PLL-PA can exhibit stable phase separation behavior even in salt solvents by introducing an aromatic ring. It was suggested that by changing the concentration conditions of the polymer, it could be applied as an intelligent material over a wide temperature range.

Using a scanning laser microscope and a stage that can be heated, I succeeded in clearly observing the formation and growth process of droplets on a scale of several micrometers in a polymer solution around the phase separation temperature. The PLL-SA system was observed to grow through the continuous formation and coalescence of minute droplets, whereas the PLL-PA system demonstrated the formation of droplets a certain size from the onset, which then underwent growth. It was confirmed that the phase separation behavior, which appeared to be the same on the scale of transmitted light intensity measurement, had its own characteristics. In DLS measurements, the phase separation behavior was measured on a smaller scale from the viewpoint of autocorrelation coefficient and temperature by performing measurements while increasing the temperature. In PLL-SA, the autocorrelation coefficient decreased continuously as the temperature increased, but in the PLL-PA system, the autocorrelation coefficient decreased significantly after reaching the phase separation temperature. PLL-SA changed continuously without reaching the phase separation temperature, suggesting that some structural changes may have occurred before droplet formation. While the exact minimum size of emerging PLL-SA droplets remains undetermined, drawing parallels to the dimensions of biological droplets, such as vesicles and lipid droplets, allows us to hypothesize that similar pre-formation structural

changes could be detectable. Together with the observation results using a laser microscope, it was suggested that the phase separation and droplet formation mechanisms of PLL-SA and PLL-PA may be due to different effects. This contrast not only highlights the compositeity of polymer behavior in response to temperature changes but also underscores the potential for diverse applications of these materials based on their unique phase separation dynamics.

Following our preliminary observations, I engaged in USAXS/SAXS measurements to investigate the phenomena on a nanoscale level. These measurements aimed to validate our hypotheses regarding pre-droplet formation changes by identifying specific patterns or data indicative of such alterations. In the analysis of correlation length and temperature, the phase separation behavior was considered to be a phase transition at a critical point because the correlation length diverged in both cases. Analysis in the SAXS region shows that droplet formation occurs concurrently with phase separation temperature and the divergence of the correlation length. This suggests that the continuous decrease in the autocorrelation function observed in DLS might be attributed to minute structural changes, distinct from droplet formation. Moreover, our multi-scale measurement results elucidate a notable stability in the phase separation behavior of the PLL-PA system, contrasting with PLL-SA. Despite observable changes surrounding the phase separation temperature in PLL-PA, no continuous alterations were detected, underscoring a fundamental difference in the phase separation dynamics between the two polymers.

To further delineate the observed trend in phase separation behavior, neutron scattering experiments were conducted under controlled conditions, ensuring the phase separation temperatures of PLL-SA and PLL-PA remained constant. These experiments revealed a change in the hydration structure factor with water molecules in PLL-SA before and after the phase separation temperature. However, the significance of this observation towards clarifying the

underlying mechanism is tempered by the potential influence of varying polymer concentrations within the measurements.Contrastingly, the phase separation behavior of PLL-PA demonstrated remarkable stability across different scales of measurement. This stability is attributed to the π-π interactions facilitated by the aromatic ring incorporated for enhancing phase separation under physiological conditions. Typically, electrostatic interactions between amino and carboxyl groups are expected to predominate over π-π interactions. This unexpected finding prompts a reevaluation of the conditions under which hydrophobic groups, capable of engaging in π-π interactions, are introduced. Such a reassessment could elucidate the balance of interactions that contribute to the stabilization of phase separation behavior in PLL-PA.

2-6 References

1. McNaught, K. S. P. & Olanow, C. W. Protein aggregation in the pathogenesis of familial and sporadic Parkinson's disease. Neurobiology of Aging vol. 27 530–545 Preprint at https://doi.org/10.1016/j.neurobiolaging.2005.08.012 (2006).
2. Ross, C. A. & Poirier, M. A. Protein aggregation and neurodegenerative disease. Nat Med 10, S10 (2004).
3. Uversky, V. N. Intrinsically disordered proteins in overcrowded milieu: Membrane-less organelles, phase separation, and intrinsic disorder. Current Opinion in Structural Biology vol. 44 18–30 Preprint at https://doi.org/10.1016/j.sbi.2016.10.015 (2017).
4. Alberti, S. & Dormann, D. Liquid-Liquid Phase Separation in Disease. (2019) doi:10.1146/annurev-genet-112618.
5. Lee, S. & Kim, H.-J. Prion-like Mechanism in Amyotrophic Lateral Sclerosis: are Protein Aggregates the Key? Exp Neurobiol 24, 1–7 (2015).
6. Hyman, A. A., Weber, C. A. & Jülicher, F. Liquid-liquid phase separation in biology. Annual review of cell and developmental biology vol. 30 39–58 Preprint at https://doi.org/10.1146/annurev-cellbio-100913-013325 (2014).
7. Das, S., Eisen, A., Lin, Y. H. & Chan, H. S. A Lattice Model of Charge-Pattern-Dependent Polyampholyte Phase Separation. Journal of Physical Chemistry B vol. 122 5418–5431 Preprint at https://doi.org/10.1021/acs.jpcb.7b11723 (2018).
8. Langer, R. Biomaterials in drug delivery and tissue engineering: One laboratory's experience. Acc Chem Res 33, 94–101 (2000).
9. Holzapfel, B. M. et al. How smart do biomaterials need to be? A translational science and clinical point of view. Advanced Drug Delivery Reviews vol. 65 581–603 Preprint at https://doi.org/10.1016/j.addr.2012.07.009 (2013).

10. Kanazawa, R., Sasaki, A. & Tokuyama, H. Preparation of dual temperature/pH-sensitive polyampholyte gels and investigation of their protein adsorption behaviors. Sep Purif Technol 96, 26–32 (2012).

11. Lutz, J. F., Akdemir, Ö. & Hoth, A. Point by point comparison of two thermosensitive polymers exhibiting a similar LCST: Is the age of poly(NIPAM) over? J Am Chem Soc 128, 13046–13047 (2006).

12. Fu, Y. & Kao, W. J. Drug release kinetics and transport mechanisms of non-degradable and degradable polymeric delivery systems. Expert Opinion on Drug Delivery vol. 7 429–444 Preprint at https://doi.org/10.1517/17425241003602259 (2010).

13. Matsarskaia, O. et al. Phase-Separation Kinetics in Protein-Salt Mixtures with Compositionally Tuned Interactions. Journal of Physical Chemistry B 123, 1913–1919 (2019).

14. Wang, M. et al. Binary solvent colloids of thermosensitive poly(N - isopropylacrylamide) microgel for smart windows. Ind Eng Chem Res 53, 18462–18472 (2014).

15. Chu, L.-Y., Park, S.-H., Yamaguchi, T. & Nakao, S.-I. Preparation of Thermo-Responsive Core-Shell Microcapsules with a Porous Membrane and Poly(N-Isopropylacrylamide) Gates. Journal of Membrane Science vol. 192 (2001).

16. Kawaguchi, S. et al. High-throughput powder diffraction measurement system consisting of multiple MYTHEN detectors at beamline BL02B2 of SPring-8. Review of Scientific Instruments 88, (2017).

17. Nishibori, E. et al. The Large Debye-Scherrer Camera Installed at SPring-8 BL02B2 for Charge Density Studies. Nuclear Instruments and Methods in Physics Research A (2001).

18. Hattori, T., Suzuki, K., Miyo, T., Ito, T. & Machida, S. Development of 0.5 mm gauge size radial collimators for high-pressure neutron diffraction experiments at PLANET in J-PARC. Nucl Instrum Methods Phys Res A 1059, (2024).

19. Ikeda, K. et al. Local structural changes in V–Ti–Cr alloy hydrides with hydrogen absorption/desorption cycling. Int J Hydrogen Energy 51, 79–87 (2024).

20. Gao, Y. et al. A cyclic voltammetric technique for the detection of micro-regions of bmimPF6/Tween 20/H2O microemulsions and their performance characterization by UV-Vis spectroscopy. Green Chemistry 8, 43–49 (2006).

21. Wright, S. F., Zadrazil, I. & Markides, C. N. A review of solid–fluid selection options for optical-based measurements in single-phase liquid, two-phase liquid–liquid and multiphase solid–liquid flows. Experiments in Fluids vol. 58 Preprint at https://doi.org/10.1007/s00348-017-2386-y (2017).

22. Das, E. & Matsumura, K. Tunable phase-separation behavior of thermoresponsive polyampholytes through molecular design. J Polym Sci A Polym Chem 55, 876–884 (2017).

23. Rajan, R., Pangkom, N. & Matsumura, K. Design of Stimuli-Responsive Polyampholytes and Their Transformation into Micro-Hydrogels for Drug Delivery. in ACS Symposium Series vol. 1350 47–62 (American Chemical Society, 2020).

24. Kang, H. et al. Ultrafast deactivation mechanisms of protonated aromatic amino acids following UV excitation. Physical Chemistry Chemical Physics 394–398 (2005) doi:10.1039/b414986f.

25. Moellering, E. R. & Benning, C. RNA interference silencing of a major lipid droplet protein affects lipid droplet size in Chlamydomonas reinhardtii. Eukaryot Cell 9, 97–106 (2010).

26. Wilfling, F., Haas, J. T., Walther, T. C. & Jr, R. V. F. Lipid droplet biogenesis. Current Opinion in Cell Biology vol. 29 39–45 Preprint at https://doi.org/10.1016/j.ceb.2014.03.008 (2014).

27. Wolins, N. E., Brasaemle, D. L. & Bickel, P. E. A proposed model of fat packaging by exchangeable lipid droplet proteins. FEBS Letters vol. 580 5484–5491 Preprint at https://doi.org/10.1016/j.febslet.2006.08.040 (2006).

28. Osaka, N., Shibayama, M., Kikuchi, T. & Yamamuro, O. Quasi-elastic neutron scattering study on water and polymer dynamics in thermo/ pressure sensitive polymer solutions. Journal of Physical Chemistry B 113, 12870–12876 (2009).

29. Huse, D. A. & Fisher, D. S. Dynamics of Droplet Auctuations in Pure and Random Ising Systems. PHYSICAL REVIEW B vol. 35 (1987).

30. Iiyama, T., Ruike, M. & Kaneko, K. Structural Mechanism of Water Adsorption in Hydrophobic Micropores from in Situ Small Angle X-Ray Scattering. www.elsevier.nl/locate/cplett.

31. Benedek, G. B., Lastovka, B., Giglio, M., Stauffer, D. & Kiangt, C. S. Cannell, in Critical Phenomena. ^R. D. Mountain, Rev. Mod. Phys vol. 27 (1971).

32. Wut, D. Q., Chug, B., Lundberg, R. D. & Macknight, W. J. Small-Angle X-Ray Scattering (SAXS) Studies of Sulfonated Polystyrene Ionomers. 2. Correlation Function Analysis. Macromolecules vol. 26 (1993).

33. Singh, S. S., Aswal, V. K. & Bohidar, H. B. Structural studies of agar-gelatin complex coacervates by small angle neutron scattering, rheology and differential scanning calorimetry. Int J Biol Macromol 41, 301–307 (2007).

34. Steininger, R. & Bilgram, J. H. LIGHT SCATFERING AT THE SOLID-LIQUID INTERFACE OF CYCLOHEXANE. Journal of Crystal Growth vol. 99 (1990).

35. Wu, X. et al. Promoted liquid-liquid phase separation of PEO/PS blends with very low LiTFSI fraction. Polymer (Guildf) 260, (2022).

36. Moore, E. B. & Molinero, V. Growing correlation length in supercooled water. Journal of Chemical Physics 130, (2009).

37. Kurita, R. & Tanaka, H. Critical-like phenomena associated with liquid-liquid transition in a molecular liquid. Science (1979) 306, 845–848 (2004).

38. Kumar, P. et al. Glass transition in biomolecules and the liquid-liquid critical point of water. Phys Rev Lett 97, (2006).

Chapter 3

Application of DDS by polyampholytes

3-1 Introduction

In Chapter 2, we focused on the liquid-liquid phase separation behavior of ampholyte polymers and compared the behavior on multiple scales by conducting and evaluating measurements at different scales. This chapter focuses on the high biocompatibility and temperature responsiveness of ampholyte polymers and describes their application as carriers in drug delivery systems.

Many of the materials that have been studied in recent years as carriers of DDS are materials with functions and properties called smart materials or intelligent materials[1-5]. Stimuli-responsive polymers are one type of such polymers, and as mentioned in Chapter 1, temperature-responsive polymers[6-8] such as PLL-SA and PLL-PA are also being studied in the DDS field as temperature-responsive carriers.

The high reactivity to thermal stimuli required of conventional temperature-responsive carriers stems from the fact that it is difficult to continue stably supplying heat from outside the body due to the homeostatic function of the living body[9, 10]. It is extremely difficult to continuously supply heat to the in-vivo environment around the carrier precisely in 1°C increments due to external stimuli. Therefore, one of the goals of conventional temperature-responsive carriers was how quickly and sharply they could respond to temperature changes. Although many studies have been reported on overcoming challenges through precision synthesis of polymers[11, 12], etc., I thought it would be effective to first design a carrier that is not affected by the homeostatic functions of the organism and that can utilise temperature responsiveness.

I hypothesised that the primary challenge associated with the application of temperature-responsive polymers in DDS, which is their high sensitivity to fluctuating thermal stimuli, could be effectively addressed by designing composite materials. These composites would integrate materials with diverse properties, enabling a self-regulating mechanism rather than relying on

external control for drug delivery. Near-infrared light is appropriate as a source of heat generation by light stimulation because of its high penetration into living organisms and its use in medical practice[13, 14]. Therefore, materials with a photothermal effect on near-infrared light were applied in this study.

Many metallic nanoparticles have been reported as materials with photothermal effects, with gold nanoparticles being a typical example. Gold nanoparticles absorb near-infrared light and are used as heat-generating materials in thermotherapy[15-17]. Metals such as gold and silver are characterised by their ability to produce particles with well-defined diameters and allow easy surface modification. Liquid metals (LMs) are also a type of metal nanoparticles that show photothermal effect with near-infrared light[18-23]. Mercury, a typical LM, has several excellent mechanical properties, including high electrical conductivity and flexibility, but it is also known to have high biotoxicity. However, gallium-based LMs, which have been attracting attention in recent years, are chemically stable and have extremely low biotoxicity in addition to the properties of conventional LMs. Furthermore, compared to other solid metals such as gold and silver nanoparticles, gallium-based LMs have a lower melting point, which makes it easier to break the oxide film formed on the metal surface and transform it into particles[20, 23]. Particulation can also be achieved by a simple method such as sonication, which is ideal for processing composite materials.

The LM temperature-responsive polymer composite is a physical, stimulus-responsive carrier, triggered by light. In this Chapter, the anticancer drug doxorubicin hydrochloride (DOX), was selected as the drug to be delivered, assuming that it is particularly suitable for anticancer drug therapy in spite of strong side effects. DOX is a widely used anticancer drug that inhibits DNA and RNA synthesis[24, 25]. Combined with near-infrared laser therapy, it is expected to exert its effects locally at the target site with minimal side effects.

Based on the above, the present study aimed to capitalise on the temperature-responsive attributes of the polyampholyte PLL-PA and harness the photofunctionality of LMs, to engineer a composite. This composite was designed to exhibit a two-step responsive behaviour—a two-step stimuli-response—wherein stable heat generation, upon triggering with near-infrared laser light, induced phase separation. Through this approach, I endeavoured to fabricate, assess, and characterise an innovative, intelligent composite entity that exhibits a sequential response mechanism.

3-2 Experiment

3-2-1 Materials

A 25% ε-polylysine solution was procured from JNC Corporation (Tokyo, Japan). Anhydrous succinic acid and anhydrous phthalic acid were obtained from Nacalai Tesque Inc. (Kyoto, Japan). The powder form of phosphate-buffered saline (PBS (-)) was purchased from Shimadzu Diagnostics Corp. (Tokyo, Japan). The Gallium-Indium eutectic alloy was employed using products from Alfa Aesar (Ward Hill, MA, USA). 2-iminothiolane hydrochloride was procured from Toronto Research Chemicals Inc. (Toronto, Canada) and doxorubicin hydrochloride was procured from Wako (Osaka, Japan).

3-2-2 Synthesis of temperature-responsive polymer

An aqueous solution of 25% PLL was prepared, and an appropriate amount of PA was added to the solution. The mixture was stirred at 60°C until complete dissolution of reagents. Fifty per cent of the amino groups of PLL carboxylated with PA, was denoted as PLL-PA50, respectively. To increase the affinity of PLL-PA with LM, 2-iminothiolane hydrochloride was added and the mixture was stirred at 25°C for 1 h. In this process, 40% of the amino group of PLL was

carboxylated with PA and 20% was thiolylated with 2-iminothiolane hydrochloride (PLL-PA-(SH)). The polymer solution obtained was lyophilised and stored in vacuum until usage.

3-2-3 Characterization of the polyampholyte

The synthesised polymers were subjected to ^{1}H nuclear magnetic resonance (NMR) spectroscopy using a 400 MHz NMR instrument from Bruker. The NMR data acquired were analysed using the Topspin 3.6.5 software to calculate the compositional ratios based on the integration values.

The temperature responsiveness and phase separation temperature were determined using a temperature-controlled UV-Vis spectrophotometer (UV-1800, Shimadzu Corp., Kyoto, Japan). Polymer solutions were placed in 2 mL quartz cells, and optical data were collected continuously at a fixed wavelength of 550 nm, while varying the temperature. The transmitted light intensity of the homogeneous solution state prior to phase separation was set as 100%, and the temperature at which the transmitted light intensity reached 50% was defined as the phase separation temperature.

3-2-4 Particularisation of LM

Particularisation of the LM was achieved through ultrasonic treatment. Changes in particle size were observed using a transmission electron microscope (TEM) (HF-7650, Hitachi High-Tech Corp., Tokyo, Japan) to assess the effects of processing time and thiol functionalisation. Microgrids (NS-C15, Stem, Tokyo, Japan) were utilised for the observations. A diluted sample solution was deposited onto the grid with a droplet, dried at 50°C, washed with distilled water for salt removal, and subsequently dried again in an oven.

3-2-5 Characterisation of composites

Confirmation of the photothermal effect of the composite and verification of control were performed by irradiating 1 ml of sample solution in a cell with a laser beam with a wavelength of 785 nm (BRM-785-1.0-100-0.22-SMA; B&W Tek, Newark, DE, USA, 6.29 W/cm^2), taking thermographic (FLIR i7: FLIR Systems) images, and evaluating with a thermocouple thermometer (AD-5601A: A&D Company, Tokyo, Japan).

The two-step reaction was observed using a laser scanning microscope (IX73: Olympus, Tokyo, Japan), by placing a droplet of the sample solution on a glass slide, covering it with a coverslip, and irradiating it with 808 nm laser light for 3 s.

DOX dissolved in PBS was used as the solvent in the polymer solution preparation, and the composite sample was prepared by adding LM followed by sonication, as described previously. The sample solution was adjusted to phase separation at 41°C, and the final concentration of DOX was calculated using a calibration curve.

The release rate of DOX was determined by irradiating a 1 mL sample solution in a cell with 808 nm laser light (LSR808-5W-FCH: LASEVER) for 3 min, to induce phase separation (15.3 W/cm^2). The concentrations of DOX in the upper and lower phases were calculated based on the calibration curve obtained, using a microplate reader (Infinite 200 PRO M Nano+: Tecan, Männedorf, Switzerland) at 480 nm.

3-2-6 Cell viability assay

To assess the functionality of the composites and the efficacy of drug action, an 3-(4,5-dimethylthiazol-2-yl)-2,5-diphenyltetrazolium bromide (MTT) assay was performed. The polymer concentration was adjusted and fixed at 25 wt% to achieve phase separation at 41°C.

Composites were prepared either containing DOX (1 μg/mL) or without DOX. Cytotoxicity was compared with and without laser irradiation (808 nm, 3 W, 5 min) (15.3 W/cm^2).

Human colon adenocarcinoma HT-29 cells (from DS Pharma Biomedical (Tokyo, Japan)) were cultured and 500 μL of cell suspension was added to 24-well plates at a density of 6000 cells/mL. After 60 h of incubation, the samples (500 μL) were added, followed by laser irradiation and continued incubation. After 3, 6, and 24 h, samples were removed, and residual samples were washed with PBS. Subsequently, MTT solution dissolved in DMEM without foetal bovine serum (FBS), at a concentration of 100 μg/mL, was added in 500 μL aliquots and incubated for 4 h. The liquid was then removed, and 500 μL of DMSO was added. To completely remove the LM, the solution obtained was transferred to microtubes and subjected to centrifugation (20°C, 1000 rpm, 5 min), and the resulting supernatants were transferred to a 96-well plate, in 100 μL aliquots, for measurement using a microplate reader (λ = 540 nm).

3-3 Results and discussion

3-3-1 Characterization of temperature-responsive polymer

The temperature-responsive polyampholyte PLL-PA(-SH) was synthesised by adding 2-iminothiolane hydrochloride to PLL-PA and expanding at 25 °C for 1 h according to Scheme 2. Degree of substitution was calculated from integration values using ^{1}H NMR spectroscopy (Figure 19 and Table3).

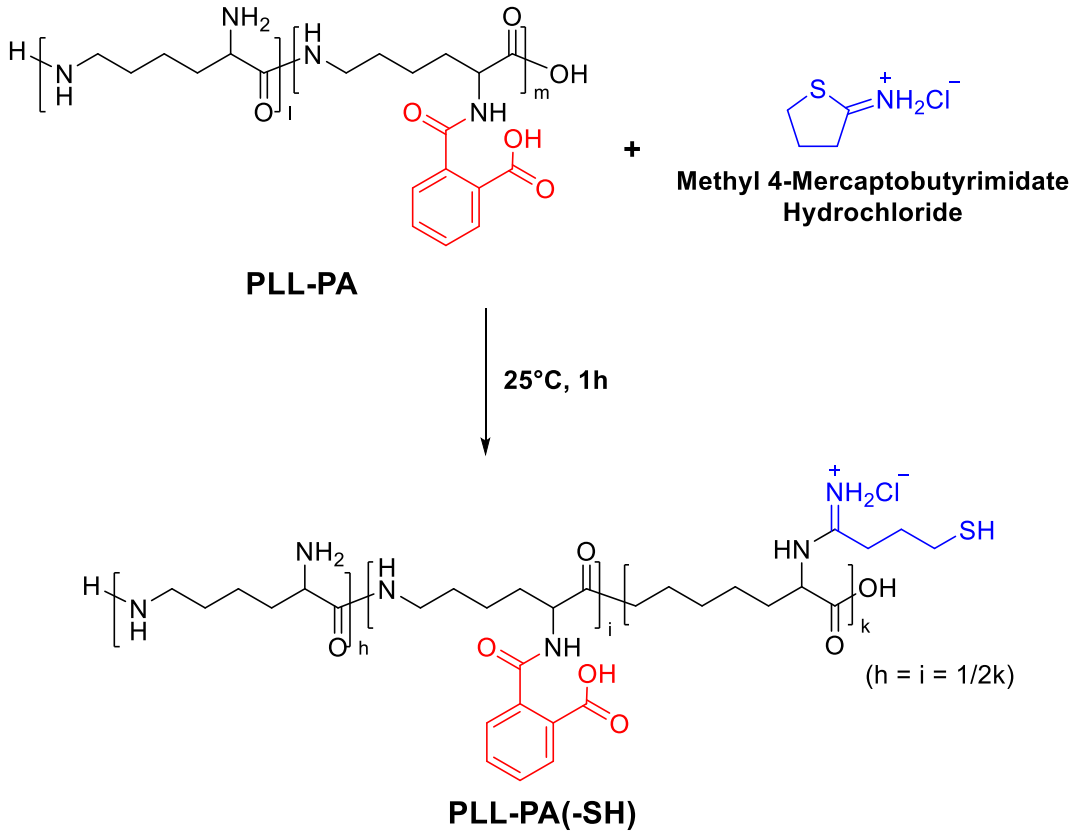

Scheme 2 Synthesis of PLL-PA(-SH)

$$2 - IT(\%) = \frac{\frac{[1]}{2}}{\frac{\delta}{6} + PA(\%) + \frac{[1]}{2}} \times 100$$

Table 3 Characterization of polyampholytes

	composition			composition		
PLL	100	0	0	100	0	0
PLL-PA(-SH)	40	40	20	40	42	18

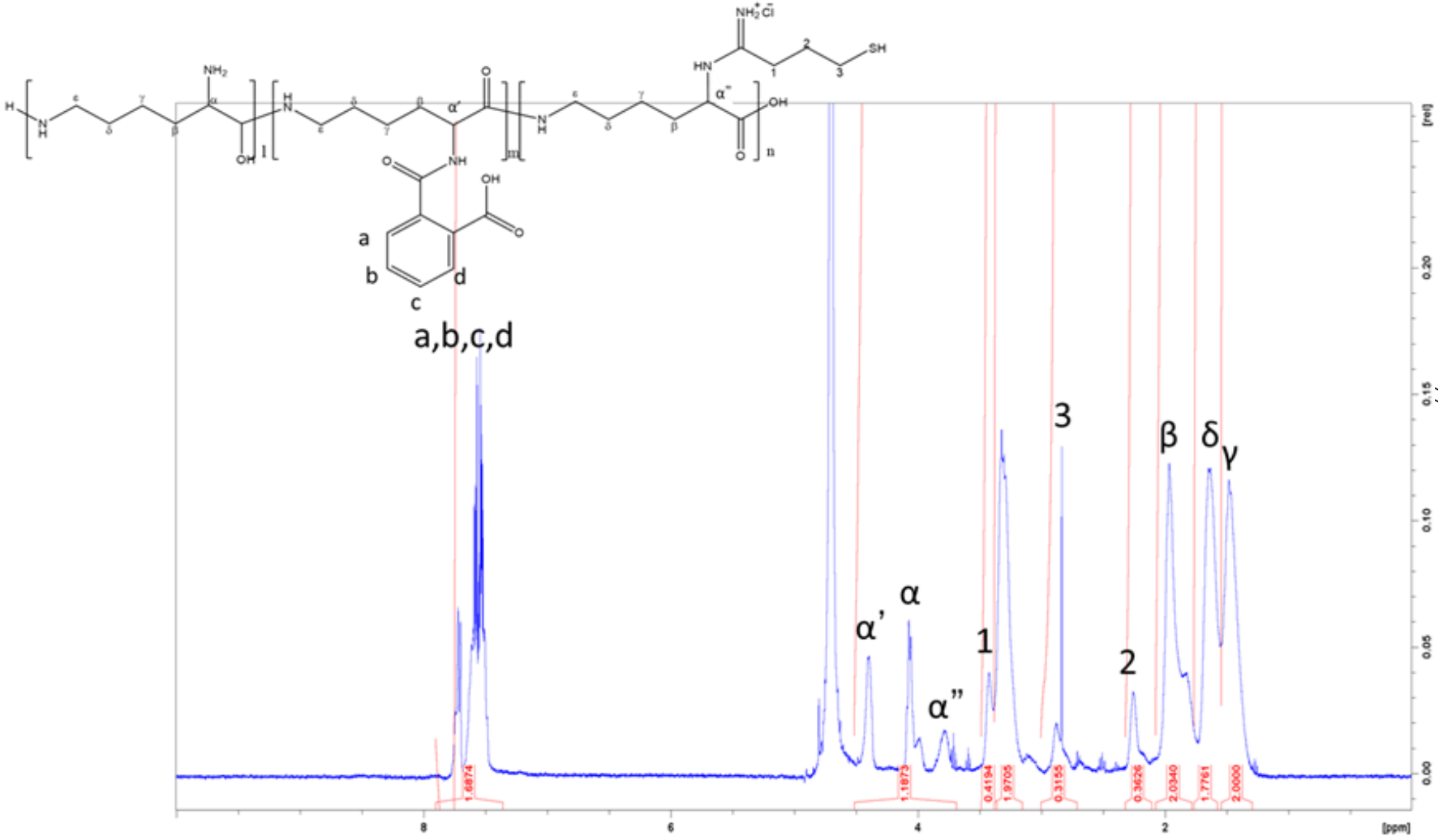

Figure 19 ^{1}H-NMR of PLL-PA50(solvent：D_2O)

The introduction ratio of anions can be easily varied by adjusting the feeding amounts of PA. In order to obtain phase separation temperatures relevant for biomaterial applications, an introduction ratio in the range of 40-60% is considered suitable. When utilised as carriers in this study, polymers in a state where the ratio of anions (-COOH) to cations (-NH2) was equimolar were synthesised and employed for PLL-PA(-SH), PLL to PA to SH ratio of 40:40:20).

To assess the temperature responsiveness of PLL-PA(-SH) in both pure water and saline solution, we conducted measurements of transmitted light intensity using a temperature-variable UV-Vis spectrophotometer.

The same behaviour was confirmed for PLL-PA(-SH) (Figure 20). The phase separation temperature curves obtained from these experiments confirm the presence of LCST-type phase separation and demonstrate that the phase separation temperature can be tuned over a wide range by adjusting polymer concentration.

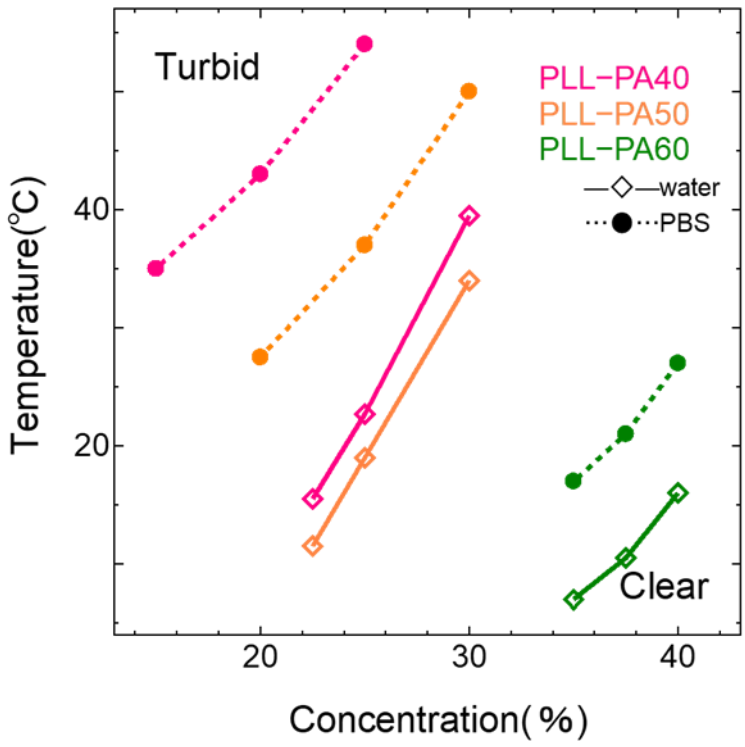

Figure 20 Phase separation curves of PLL-PA at 40-60% PA incorporation in water and PBS.

The phase-separation behaviour of PLL-PA(-SH) in salt solutions is thought to be due to the π-π interactions caused by the introduction of the benzene ring. I also confirmed that the phase separation temperature decreased at the same concentration, as more hydrophobic moieties were introduced (Figure 21). This could be due to the fact that the main phase separation behaviour is caused by the electrostatic interaction between the amino and carboxyl groups, whereas an excess of anionic carboxyl groups causes an imbalance in the interaction.

These results confirm that PLL-PA(-SH) are polyampholytes capable of stable phase separation at salt concentrations encountered in physiological conditions; this is necessary for temperature-responsive biomaterials.

With cancer treatment as the target application, I decided to employ PLL-PA(-SH) with a 25 wt% polymer concentration and a phase separation temperature of 41°C as the designated DDS carrier.

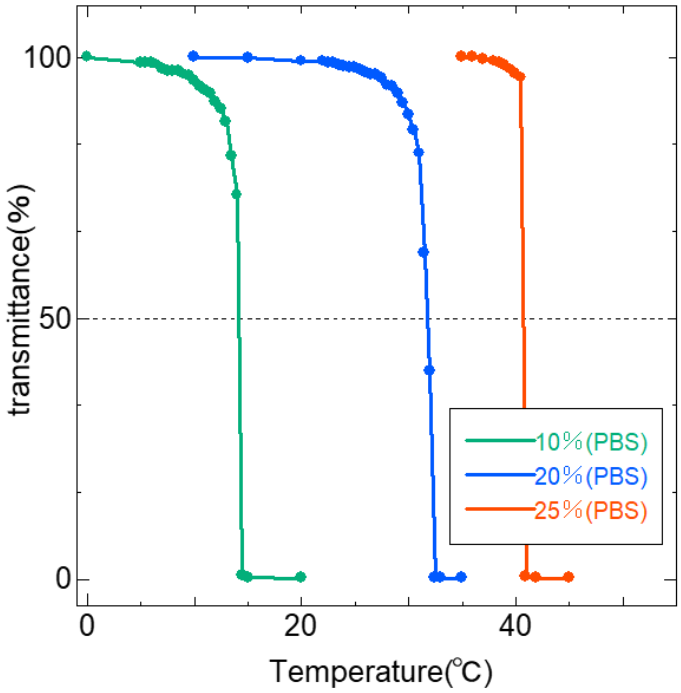

Figure 21 Changes in transmittance intensity across different temperature ranges (UV-vis, λ=550 nm; 50% transmittance indicates phase separation temperature) The phase separation temperatures for PLL-PA(-SH) at various concentrations in PBS.

3-3-2 Fabrication of compositees

As the next step, I explored the optimal conditions for the particle formation of the LM, the other component of the composite. LM was added to a polymer solution (10 ml) adjusted to the optimal concentration, and variations in conditions were introduced through sonication. Pulsed sonication was chosen due to the simplicity of the method and uniformity in the particle size achieved during particle formation for composite preparation. The changes in particle size by sonication time and the dispersion effect resulting from thiolation of the polymer were evaluated by TEM observation of the composite after sonication with a 10-fold dilution (Figure 22). The results showed that relatively large-sized LM nanoparticles (LMNPs) with sizes ranging from 200 to 500 nm were obtained with a sonication time of 5 min (Figure22(A)). By extending the

sonication time to 10 min (Figure 22(B)), a reduction in the particle size of LMNPs to 200-100 nm was confirmed. Since heat generation during sonication in pulse mode, can cause potential thermal damage to the polymer, a sonication time of 10 min was deemed appropriate in this study. However, for both sonication times, aggregation of LMNPs was observed more frequently with PLL-PA50 than without PLL-PA50.

The effect of thiolation on the polymer, to increase the affinity as a composite, was evaluated by preparing a similar sample using PLL-PA(-SH) (Figure 22(C)). Although the average particle size was 200-100 nm, more monodisperse particles were observed compared to the PLL-PA50 sample, and smaller monodisperse particles were observed even when the duration of sonication was same. The findings indicate that the addition of thiol groups improves the dispersibility of LMNPs, underscoring the benefits of thiolation in the preparation of the composite.

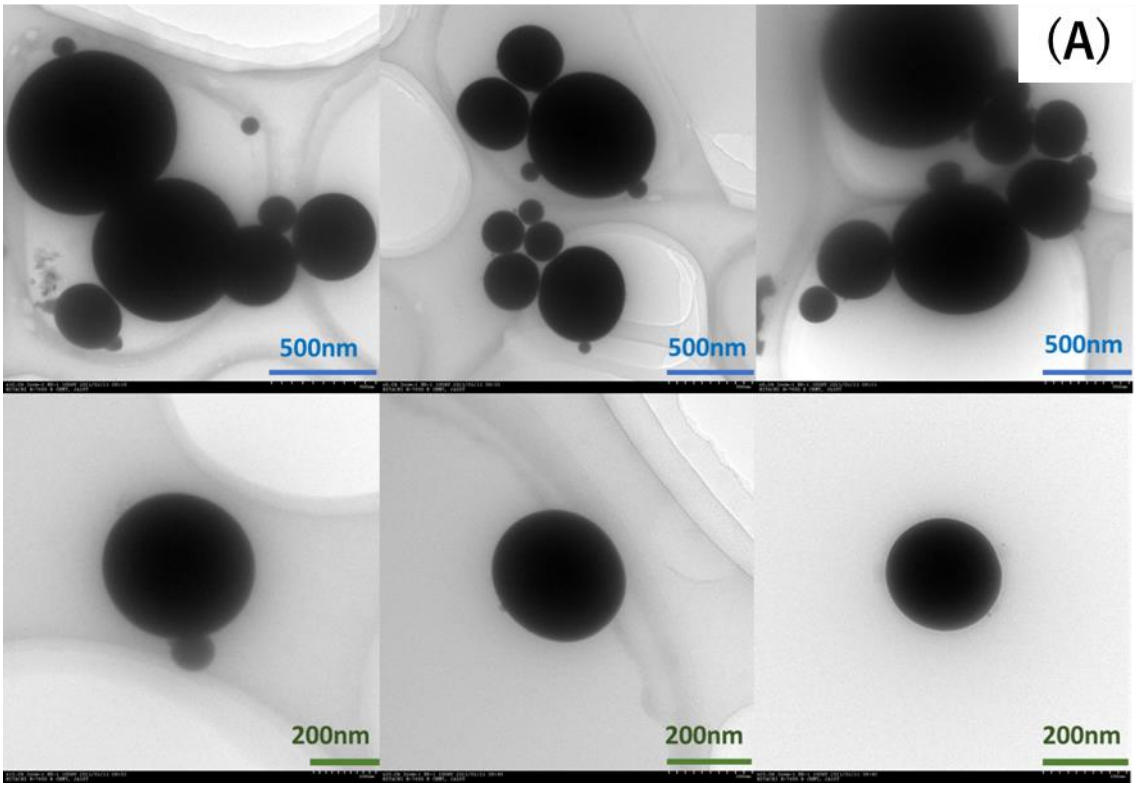
(A)
500nm
500nm
500nm
200nm
200nm
200nm

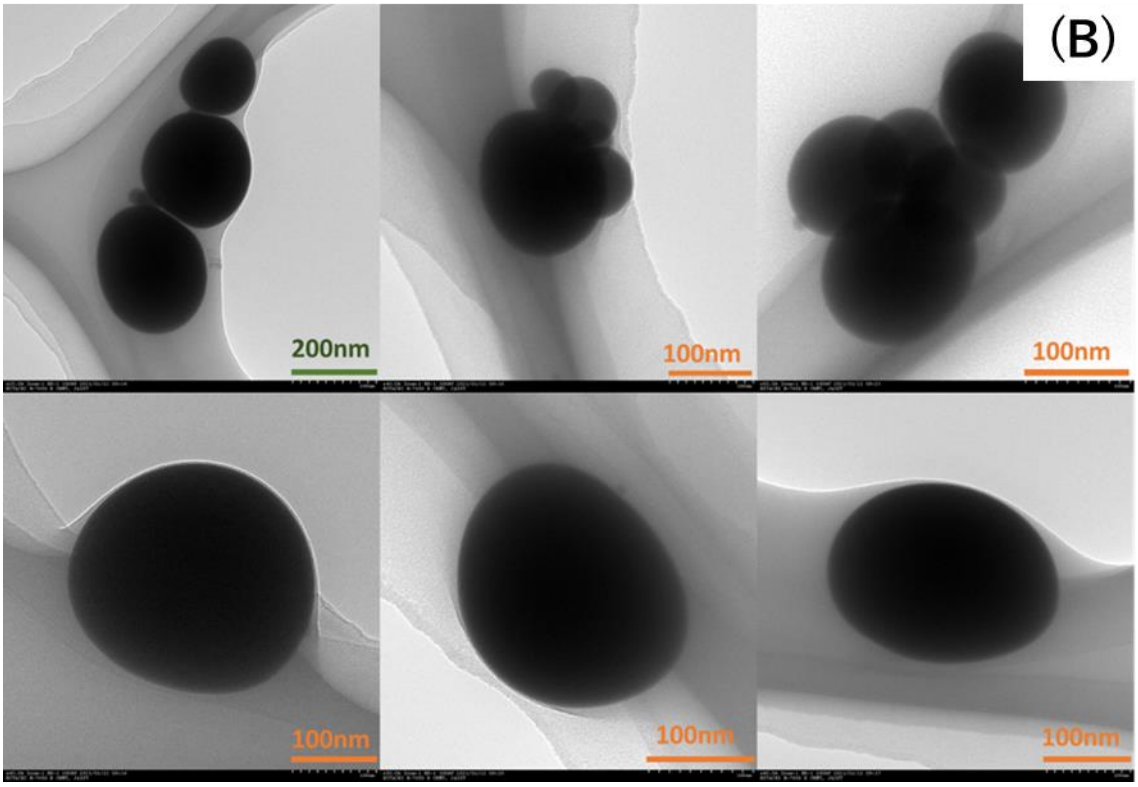
(B)
200nm
100nm
100nm
100nm
100nm
100nm

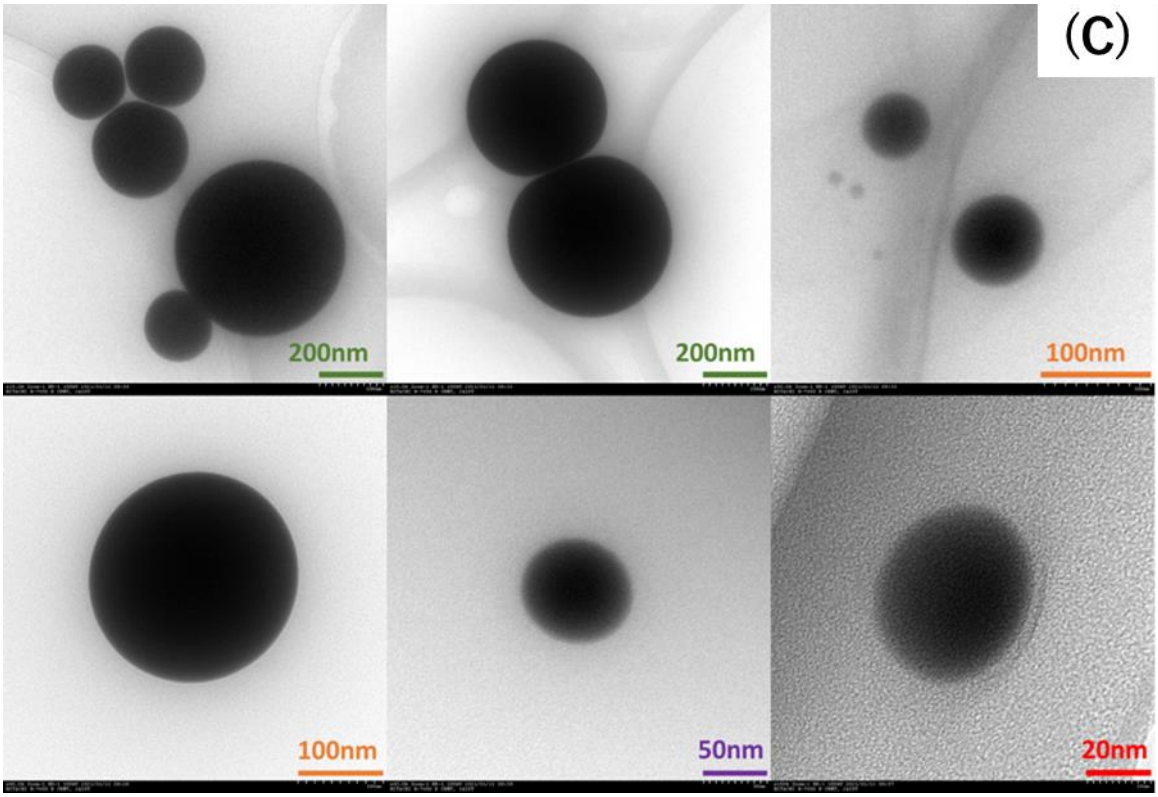

(Figure 22) TEM images demonstrating LM nanoparticle formation and thiolation via pulse sonication with 2 seconds of irradiation per pulse (20 kHz, Ice Bath, 10 ml Polymer, 30 µL LM): (A) 5-min on PLL-PA50, (B) 10-min on PLL-PA50, (C) 10-min on PLL-PA(-SH)

3-3-3 Characterisation of composites

Following the assessment of the compatibility between the polymer and LM for use as a composite, I further characterised the composite as such. Exploration of the photo-thermal characteristics of the composite and its control was carried out through thermographic measurements (Figure 23(A)) and thermal cycling (Figure 23(B)).

The thermographic images in figure 23(A) show results of the composite being heated by irradiation with a near-infrared laser (λ = 785 nm). In the control PBS solution in the upper panel, the temperature increased by only 1.8°C after 3 min of irradiation. However, the temperature of the composite solution increased by 5.5°C after 3 min of irradiation.

In figure 23(B), a 96-well plate containing 100 μL each of PBS solution and composite, was irradiated with the same near-infrared laser for each well, and the change in temperature was recorded using a thermocouple thermometer. The rate of change in temperature at each elapsed time was measured (Figure 23B-1). The results indicate almost no correlation between the laser irradiation time and the rate of temperature increase in the PBS solution, but a clear correlation in the composite containing LM. Fig. 23B-2 shows the thermal cycles of repeated irradiation and cooling, for the composite irradiated with different laser outputs. The range of temperature rise in the cycles were 2.8 ± 0.12 °C, 5.6 ± 0.41°C and 7.9 ± 0.62°C, with laser outputs of 250, 500 and 1000 nW, respectively. The high reproducibility suggests that the durability of the material and temperature can be controlled by the power photo-thermal characteristics of the composite and effectiveness of laser output and irradiation time on control and confirm the sufficient heat resistance of the material.

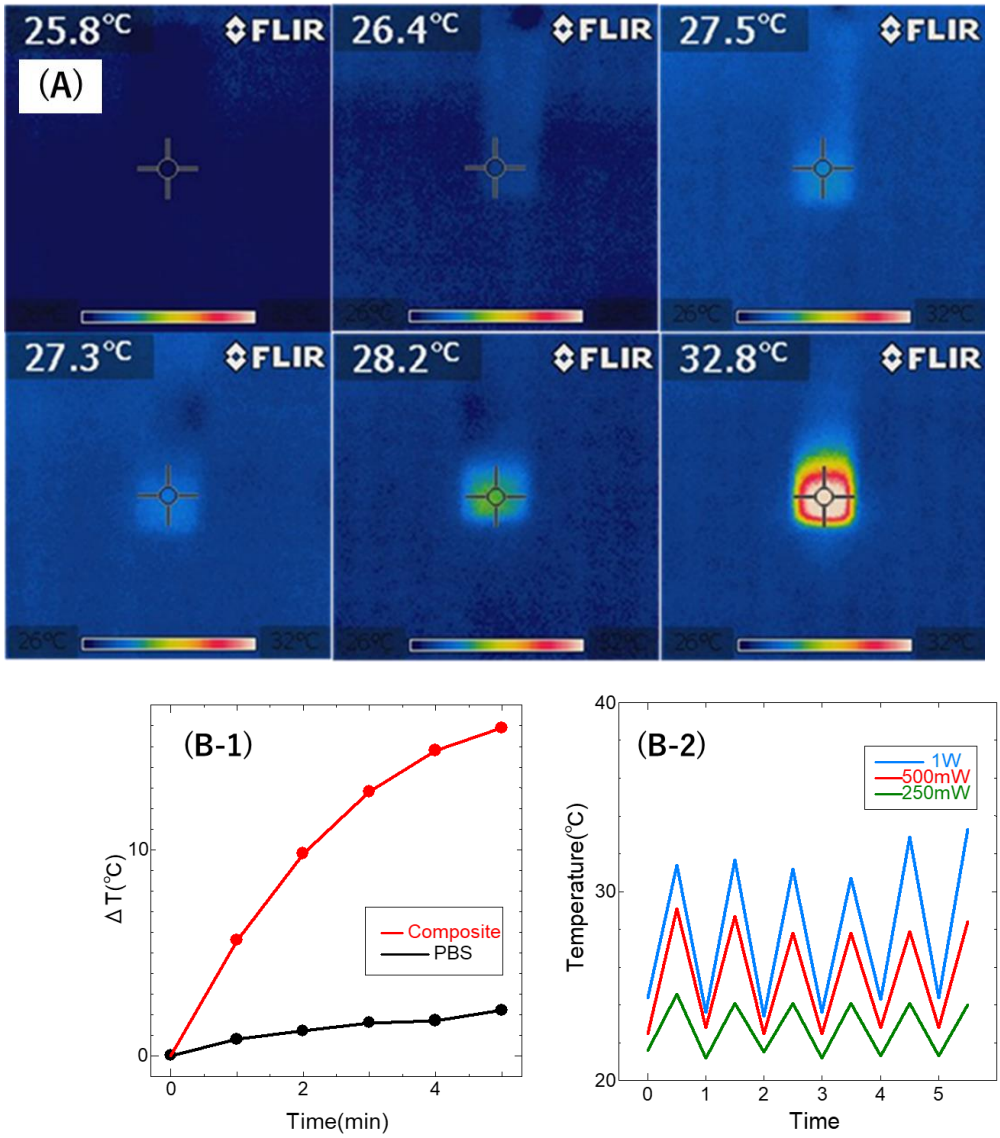

Figure 23 Characterisation of the photo-thermal properties of the composite under near-infrared laser (λ=785 nm) exposure: (A) Thermography images: top row - PBS solution (1 mL), bottom row - composite (1 ml) at 0, 1 and 3 min of irradiation. (B) Temperature changes in samples (PBS or composite) in a 96-well plate measured via thermocouple: (B-1) Temperature variations for both samples during irradiation, and (B-2) Thermal cycling of the composite across 5 cycles at different power levels.

Next, I investigated if the polymer solution component could undergo liquid-liquid phase separation by utilising the heat generated through the photothermal characteristics as a carrier for DDS. Using laser microscopy, I observed the behaviour of the composite material in real-time during laser irradiation (Figure 24). For understanding the core-shell formation of the composite, I also studied samples involving the addition of LM to a thiol-bearing, 16-mercaptohexadecanoic acid (MHDA) solution, followed by ultrasonic treatment. While the MHDA solution exhibited slight changes around LMNPs due to laser irradiation, no further changes were observed. Conversely, in the case of the composite, a behaviour was distinctly observed as LMNPs generated heat in response to near-infrared laser light, triggering core-shell formation of the polymer solution around the particles, which then spread. As a result, I confirmed that the composite heated by near-infrared laser exhibited an increase in the overall temperature as the irradiation time was prolonged. The results from laser microscopy indicate the capability to capture the initial-stage changes of the composite.

Based on these observations, I confirmed that the composite possessed a two-step responsiveness, as intended, where it generates heat in response to light stimulation and utilises this heat to induce phase separation behaviour.

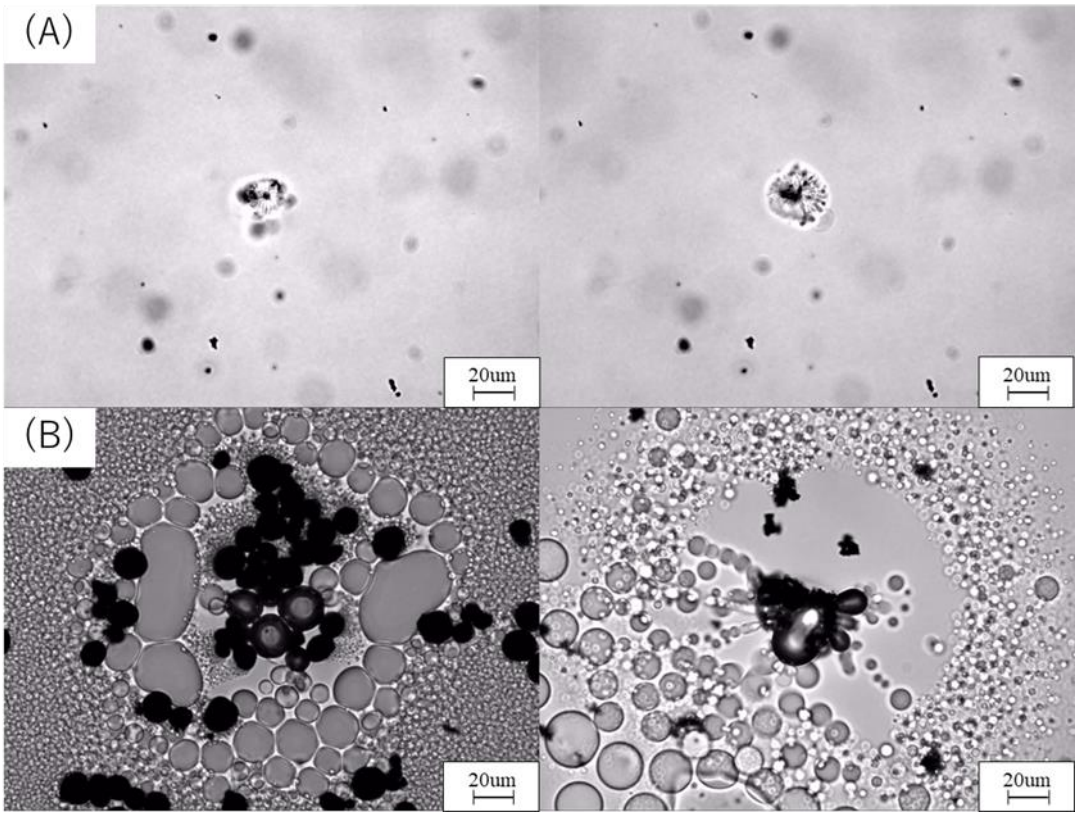

Figure 24: Laser Microscopy Images (λ=808nm, Irradiation: 3 seconds, Scale: 20 μm):

(A) MHDA + LMNPs Solution, and (B) Composite.

3-3-4 Cell viability assay

Following the confirmation of the desired properties of the composite, actual drug release experiments were conducted by adding the anticancer drug DOX, to the composite. The drug release rate was calculated by measuring three different states: the initial homogeneous state of the composite solution, the upper phase, and the lower phase after laser irradiation-induced phase separation, using a microplate reader. Due to the scattering effect caused by the presence of LMNPs, it was not feasible to directly measure the DOX concentration[26, 27]. Therefore, a polymer solution with an equivalent concentration to the composite without LM was prepared and measured for this purpose. Figure 25 shows the sample after phase separation. Due to the intricate nature of the liquid-liquid phase separation behaviour exhibited by this sample, achieving a complete separation between the upper and lower phases proved to be challenging. Compared to the DOX concentration in the homogeneous sample before phase separation, the DOX concentration in the upper phase after phase separation was about 20%, while that in the lower phase was up to 150%.

From the aforementioned results, it was evident that the composite exhibited a behaviour where it concentrated the drug in the lower phase during phase separation, rather than releasing the drug upon phase separation. This characteristic is unique, differing from that of the conventional temperature-responsive carriers designed for drug-release[6-8, 28-31]. Furthermore, given the maximum concentration enhancement factor of 1.5, I deduced that this composite holds the potential to be a carrier with reduced side effects in drug delivery applications.

By enhancing the localised concentration of the drug at the intended site, this approach affords the potential to maximise therapeutic outcomes while minimising adverse reactions when employed as a DDS carrier.

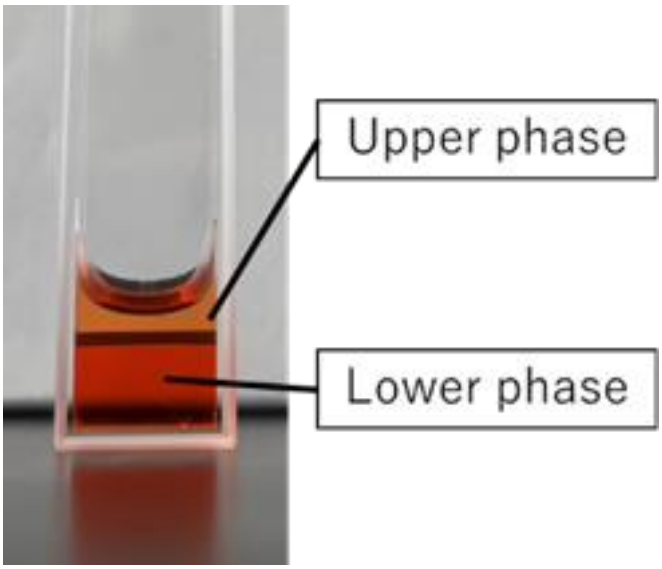

Figure 25 Composite after phase separation

Following the discovery of this capability of the composite to concentrate the drug from low concentrations for effective action, this function was evaluated for cytotoxicity using the MTT assay.

The composite was prepared at a polymer concentration of 25 wt/wt% (10 mL), an LM volume of 30 μL, and a DOX concentration of 1 μg/mL to demonstrate the phase separation temperature of 41°C. Human colon adenocarcinoma HT29 cells were used for the experiment and seeded in 24-well plates at a density of 6000 cells/ml per well and employed for the assay after 2.5 days of incubation. Experimental groups were established, including groups with and without DOX, as well as groups with and without laser irradiation (Figure 26).

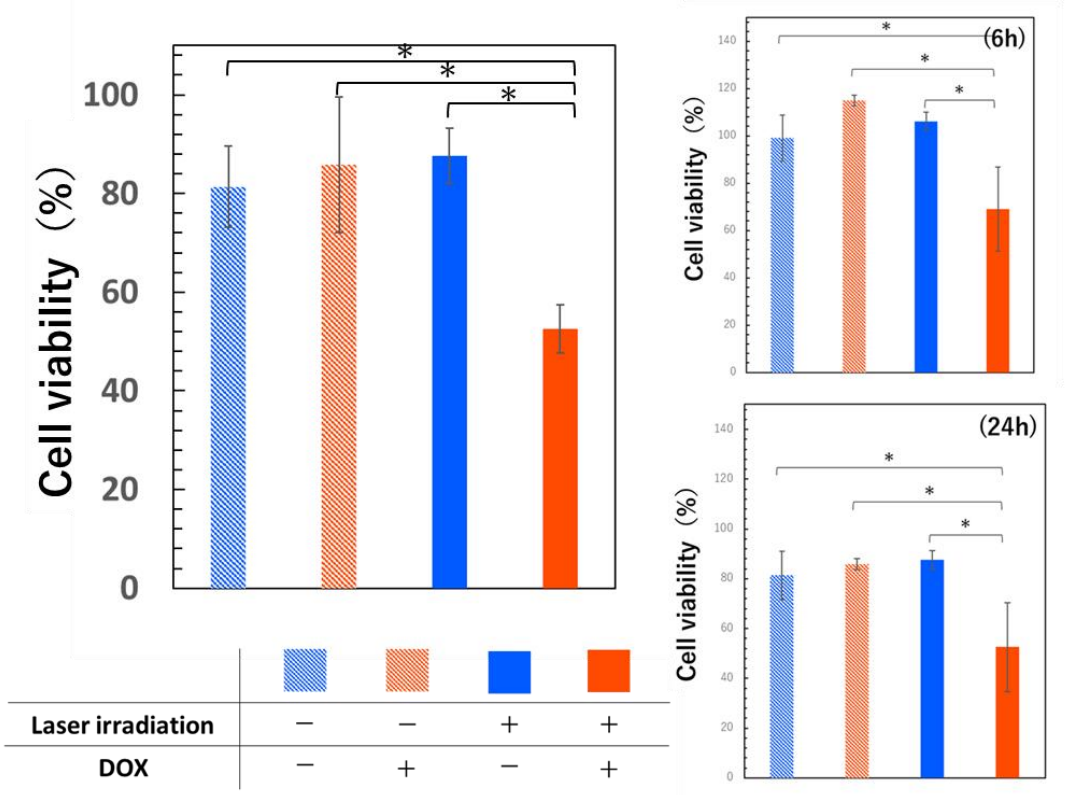

Figure 26 Results of Cell Viability Assay using MTT Assay (HT-29cells)

Significance test

Fisher's constrained LSD method

Statistically significant at 0.05 or higher

*:P<0.05

For all observed time points, the group treated with laser irradiation using the composite with DOX, exhibited the lowest cell viability. The initial DOX concentration contained in the composite was 1 μg/ml, and the lower phase DOX concentration after phase separation is thought to be a maximum of 1.5 μg/ml, due to the concentration effect. The significant toxicity at this concentration is a result consistent with previous reports[32]. There was no significant difference in cell viability between the DOX-containing group without laser irradiation and the group without DOX, suggesting that the DOX concentration of 1 μg/mL employed in this experiment was a non-toxic, low concentration for cells. The effectively higher concentration after phase separation in the irradiated Dox group may have led to this result. Furthermore, the absence of a notable difference in cell viability regardless of laser irradiation in the DOX-free group indicated that the laser output used in this experiment did not exert a substantial impact on cell viability. It can therefore, be inferred that the lower cell viability observed only in the group treated with DOX-containing composite and laser irradiation, is attributed to the property of the composite, where photothermal stimulation induced by near-infrared laser light triggered heat generation and utilised this heat for phase separation and drug concentration.

From the results of the cell viability assays, I conclude that the composite exhibits the designed functionality and effectively exerts its intended action.

3-4 Conclusion

This Chapter aimed to address the challenges in the application of conventional temperature-responsive polymers in DDS, by utilising a composite consisting of a highly biocompatible near-infrared laser-responsive LM. The composite developed in this study is an intelligent material with two-step responsiveness, possessing the unique ability to concentrate drugs. I firmly believe that this composite is a highly effective and low side-effect next-generation DDS carrier.

The phase separation temperature required for drug-release can be readily adjusted through variations in polymer concentration, and the necessary heat can be controlled via the near-infrared laser light output and irradiation time. The designed composite demonstrates the anticipated photothermal characteristics triggered by light stimulation, inducing temperature-responsive liquid-liquid phase separation. Furthermore, unlike conventional carriers, the composite concentrates the drug during phase separation, further confirmed in the cytotoxicity test.

Although challenges remain in terms of precise control over LM particle size and the phase separation temperature dependence on polymer concentration, practical applications can be enhanced. By modulating parameters like ultrasonic treatment conditions and polymer concentration, the amphiphilic properties of these polymers can be leveraged to design optimal DDS carriers in forms such as gels and micelles.

3-5 References

1. Langer, R. Biomaterials in drug delivery and tissue engineering: One laboratory's experience. *Acc Chem Res* **33**, 94–101 (2000).
2. Holzapfel, B. M. *et al.* How smart do biomaterials need to be? A translational science and clinical point of view. *Advanced Drug Delivery Reviews* vol. 65 581–603 Preprint at https://doi.org/10.1016/j.addr.2012.07.009 (2013).
3. Afshar, M., Dini, G., Vaezifar, S., Mehdikhani, M. & Movahedi, B. Preparation and characterization of sodium alginate/polyvinyl alcohol hydrogel containing drug-loaded chitosan nanoparticles as a drug delivery system. *J Drug Deliv Sci Technol* **56**, (2020).
4. Schmaljohann, D. Thermo- and pH-responsive polymers in drug delivery. *Advanced Drug Delivery Reviews* vol. 58 1655–1670 Preprint at https://doi.org/10.1016/j.addr.2006.09.020 (2006).
5. Sebeke, L. C. *et al.* Hyperthermia-induced doxorubicin delivery from thermosensitive liposomes via MR-HIFU in a pig model. *Journal of Controlled Release* **343**, 798–812 (2022).
6. Chilkoti, A., Dreher, M. R., Meyer, D. E. & Raucher, D. *T Argeted Drug Delivery by Thermally Responsive Polymers*. *Advanced Drug Delivery Reviews* vol. 54 www.elsevier.com/locate/drugdeliv (2002).
7. Sershen, S. R., Westcott, S. L., Halas, N. J. & West, J. L. *Temperature-Sensitive Polymer-Nanoshell Composites for Photothermally Modulated Drug Delivery*. *Young Investigator Award World Biomaterials Congress* (2000).
8. Bajpai, A. K., Shukla, S. K., Bhanu, S. & Kankane, S. Responsive polymers in controlled drug delivery. *Progress in Polymer Science (Oxford)* vol. 33 1088–1118 Preprint at https://doi.org/10.1016/j.progpolymsci.2008.07.005 (2008).

9. Baumgard, L. H. & Rhoads, R. P. Effects of heat stress on postabsorptive metabolism and energetics. *Annu Rev Anim Biosci* **1**, 311–337 (2013).

10. Matsarskaia, O. *et al.* Cation-Induced Hydration Effects Cause Lower Critical Solution Temperature Behavior in Protein Solutions. *Journal of Physical Chemistry B* **120**, 7731–7736 (2016).

11. Ouchi, M., Terashima, T. & Sawamoto, M. Transition metal-catalyzed living radical polymerization: Toward perfection in catalysis and precision polymer synthesis. *Chem Rev* **109**, 4963–5050 (2009).

12. Lutz, J. F., Akdemir, Ö. & Hoth, A. Point by point comparison of two thermosensitive polymers exhibiting a similar LCST: Is the age of poly(NIPAM) over? *J Am Chem Soc* **128**, 13046–13047 (2006).

13. Kobayashi, H. & Choyke, P. L. Near-Infrared Photoimmunotherapy of Cancer. *Acc Chem Res* **52**, 2332–2339 (2019).

14. Shanmugam, V., Selvakumar, S. & Yeh, C. S. Near-infrared light-responsive nanomaterials in cancer therapeutics. *Chemical Society Reviews* vol. 43 6254–6287 Preprint at https://doi.org/10.1039/c4cs00011k (2014).

15. Daraee, H. *et al.* Application of gold nanoparticles in biomedical and drug delivery. *Artificial Cells, Nanomedicine and Biotechnology* vol. 44 410–422 Preprint at https://doi.org/10.3109/21691401.2014.955107 (2016).

16. Sztandera, K., Gorzkiewicz, ;, Klajnert-Maculewicz, B. & Gorzkiewicz, M. *Gold Nanoparticles in Cancer Treatment*. http://pubs.acs.org (2018).

17. Qin, Z. & Bischof, J. C. Thermophysical and biological responses of gold nanoparticle laser heating. *Chem Soc Rev* **41**, 1191–1217 (2012).

18. Yu, Y. & Miyako, E. Manipulation of Biomolecule-Modified Liquid-Metal Blobs. *Angewandte Chemie - International Edition* **56**, 13606–13611 (2017).

19. Yu, Y. & Miyako, E. Alternating-Magnetic-Field-Mediated Wireless Manipulations of a Liquid Metal for Therapeutic Bioengineering. *iScience* **3**, 134–148 (2018).

20. Chechetka, S. A. *et al.* Light-driven liquid metal nanotransformers for biomedical theranostics. *Nat Commun* **8**, (2017).

21. Lu, Y. *et al.* Transformable liquid-metal nanomedicine. *Nat Commun* **6**, (2015).

22. Lin, Y., Liu, Y., Genzer, J. & Dickey, M. D. Shape-transformable liquid metal nanoparticles in aqueous solution. *Chem Sci* **8**, 3832–3837 (2017).

23. Ma, J. *et al.* Liquid Metal Nanoparticles as Initiators for Radical Polymerization of Vinyl Monomers. *ACS Macro Lett* **8**, 1522–1527 (2019).

24. Lv, S. *et al.* Doxorubicin-loaded amphiphilic polypeptide-based nanoparticles as an efficient drug delivery system for cancer therapy. *Acta Biomater* **9**, 9330–9342 (2013).

25. Wang, F. *et al.* Doxorubicin-tethered responsive gold nanoparticles facilitate intracellular drug delivery for overcoming multidrug resistance in cancer cells. *ACS Nano* **5**, 3679–3692 (2011).

26. Kuwata, H., Tamaru, H., Esumi, K. & Miyano, K. Resonant light scattering from metal nanoparticles: Practical analysis beyond rayleigh approximation. *Appl Phys Lett* **83**, 4625–4627 (2003).

27. Van Dijk, M. A. *et al.* Absorption and scattering microscopy of single metal nanoparticles. *Physical Chemistry Chemical Physics* **8**, 3486–3495 (2006).

28. Tiwari, G. *et al.* Drug delivery systems: An updated review. *Int J Pharm Investig* **2**, 2 (2012).

29. Siepmann, J. & Siepmann, F. Mathematical modeling of drug delivery. *International Journal of Pharmaceutics* vol. 364 328–343 Preprint at https://doi.org/10.1016/j.ijpharm.2008.09.004 (2008).

30. Khan, M. S. *et al.* Unravelling the potential of mitochondria-targeted liposomes for enhanced cancer treatment. *Drug Discovery Today* vol. 29 Preprint at https://doi.org/10.1016/j.drudis.2023.103819 (2024).

31. Fu, Y. & Kao, W. J. Drug release kinetics and transport mechanisms of non-degradable and degradable polymeric delivery systems. *Expert Opinion on Drug Delivery* vol. 7 429–444 Preprint at https://doi.org/10.1517/17425241003602259 (2010).

32. Lüpertz, R., Wätjen, W., Kahl, R. & Chovolou, Y. Dose- and time-dependent effects of doxorubicin on cytotoxicity, cell cycle and apoptotic cell death in human colon cancer cells. *Toxicology* **271**, 115–121 (2010).

Chapter 4
Summary

4-1 General Conclusion

In this thesis, I investigated PLL-PA, a polyampholyte, has both temperature responsiveness and liquid-liquid phase separation behavior. Addressing the challenge of diminished phase separation behavior in PLL-SA within salt solvents, PLL-PA was synthesized with the incorporation of a benzene ring as a hydrophobic moiety. Due to its high biocompatibility and temperature responsiveness, PLL-PA emerges as a promising candidate for applications in biomaterials such as DDS. The observed LLPS behavior of PLL-PA, a focal point of recent scientific inquiry, underscores its potential in shedding light on the mechanisms governing phase separation in polymeric systems. This thesis delves into the basic properties of PLL-PA, elucidating the mechanism of phase separation behavior, evaluating its applicability as a novel, temperature-responsive DDS carrier.

In Chapter 2, I conducted an in-depth comparative analysis of PLL-SA and PLL-PA through multi-scale measurements using to scrutinize the early stages of phase separation behavior, specifically the generation and growth of droplets. No difference was observed in the phase separation behavior of PLL-SA and PLL-PA in the measurement range beyond the transmitted light intensity measurement. However, i a detailed evaluation at various scales revealed distinct behaviors between the two polymers. As the temperature increases, PLL-SA exhibits a slight and continuous change, suggestive of structural fluctuations prior to droplet formation. On the other hand, PLL-PA showed remarkable stability in all measurements. This stability is attributed to π-π interactions, facilitated by the incorporation of aromatic rings, which promote phase separation under physiological conditions. This finding challenges the conventional expectation that electrostatic interactions between amino and carboxyl groups would predominate. The results from SAXS/USAXS measurements support this conclusion, suggesting a re-evaluation of the

conditions under which hydrophobic groups, capable of engaging in π-π interactions, are introduced into polyampholytes.

In Chapter 3, I explore the development of a novel carrier for the drug delivery system (DDS) field, utilizing the temperature-responsive properties of a composite material with photothermal properties derived from liquid metal (LM). This approach aims to address the longstanding issue of achieving a self-sufficient, stable supply of trigger stimuli for phase transitions in DDS carriers.

Our investigation involved the use of a composite carrier incorporating LM, known for its photothermal capabilities, to reliably induce phase transitions. Cell experiments demonstrated the carrier's efficacy in concentrating drugs, which implies a potential for creating DDS carriers with reduced side effects. However, achieving precise control over LM particle size and managing the phase separation temperature's dependence on polymer concentration emerged as significant challenges.

To address these challenges and enhance the practical application of our findings, I considered various modulation strategies. By adjusting ultrasonic treatment conditions and polymer concentrations, I aim to exploit the amphiphilic properties of these polymers more effectively. This approach is anticipated to facilitate the design of optimal DDS carriers, such as gels and micelles, tailored to specific therapeutic needs.

Despite the hurdles, our work lays the groundwork for future research into leveraging photothermal properties in DDS. By refining the control over material properties and exploring

the full potential of temperature-responsive carriers, I move closer to realizing more efficient, safer drug delivery mechanisms.

4-2 Achievements

-Publication-

Tomoka Hirose, Robin Rajan, Eijiro Miyako, Kazuaki Matsumura, Liquid metal-polymer nano-microconjugations as an injectable and photo-activatable drug carrier. Mol. Syst. Des. Eng., 2024, Advance Article.

-Presentation-

[International Conferences]

・**Tomoka Hirose**, Eijiro Miyako, Kazuaki Matsumura, Hybrid composites of Polyampholytes and Liquid Metals as next-generation temperature-responsive DDS carriers, The 33rd Annual Conference of the European Society for Biomaterials, Davos, Switzerland, September 2023. (Poster)

・**Tomoka Hirose,** Kazuaki Matsumura, Stabilization of polyampholytes coacervates by PEGylation during phase separation behavior, The 33rd Annual Conference of the European Society for Biomaterials, Davos, Switzerland, September 2023. (Poster）

[Domestic Conferences]

・第４３回日本バイオマテリアル学会大会、「温度応答性を持つ両性電解質高分子の液-液相分離挙動の制御および DDS 分野への応用の検討」、口頭発表、名古屋開催、令和 3 年 11 月 30 日

(https://confit.atlas.jp/guide/event/jsbabmc2021/static/outline?lang=ja)

・第 71 回高分子討論会、「温度応答性を有す両性電解質高分子の液-液相分離挙動の評価」、ポスター発表、北海道開催、令和 4 年 9 月 5-7 日(7 日発表)

(https://main.spsj.or.jp/tohron/71tohron/)

・第 44 回日本バイオマテリアル学会大会、「温度応答性両性電解質高分子の疎水性部位導入による液-液相分離挙動の評価」、ポスター発表、東京開催、令和 4 年 11 月 21-22 日(21 日発表)

(https://www.kokuhoken.jp/jsb44/)

・第 32 回日本 MRS 年次大会、「類似構造を持つ温度応答性両性電解質高分子の液-液相分離挙動の比較」、口頭発表、横浜開催、令和 4 年 12 月 5-7 日(6 日発表)

(https://www.mrs-j.org/meeting2022/jp/index.php)

・第 11 回日本バイオマテリアル学会北陸信越ブロック若手研究発表会、「両性電解質高分子の疎水性部位導入による温度応答性への影響評価」、口頭発表、オンライン開催、令和 4 年 12 月 20 日

(http://kokuhoken.net/jsbm/gyouji/gyouji20221220.html)